EDN®

JULY 2012
www.edn.com
Issue 13

Advanced power
switches boost
microhybrid
emissions gains
Page 27

Applying
the interrupt
features of MEMS
accelerometers
Page 42

IMAGE SENSORS EVOLVE TO ADDRESS
EMERGING EMBEDDED-VISION NEEDS
Page 32

Electrons prefer Coilcraft

The path of least resistance is through our new high efficiency XAL/XFL inductors

Compared to competitive parts, current zips right through our new XAL/XFL inductors.

Their DC resistance is significantly lower than other inductors of the same size. So your batteries last longer and your power supply runs cooler.

They easily handle large peak current, and their soft saturation

126% higher DCR

38% higher DCR

48% higher DCR
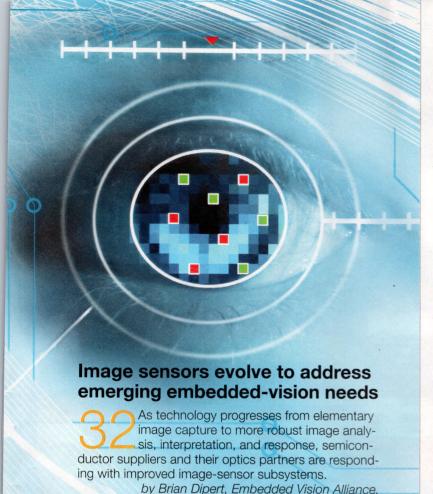
Competitors' 4.7uH inductors have much higher DCR per mm³ than Coilcraft's XAL5030.

characteristics often let you use a smaller size part without fear of overloading during transients. Built from a uniquely formulated material, XAL/XFL parts do not have the same thermal aging problems as some competitive parts.

See all the advantages of these new high efficiency inductors. Visit **coilcraft.com/xal.**

Coilcraft®

coilcraftdirect.com
No min order. Next day delivery.

WWW.COILCRAFT.COM

EDN
contents
July 2012

Image sensors evolve to address emerging embedded-vision needs

32 As technology progresses from elementary image capture to more robust image analysis, interpretation, and response, semiconductor suppliers and their optics partners are responding with improved image-sensor subsystems.

by Brian Dipert, Embedded Vision Alliance, and Eric Gregori and Shehrzad Qureshi, BDTI

Applying the interrupt features of MEMS accelerometers

42 Understand how to implement reliable and robust interrupt-based applications using MEMS-based accelerometers.

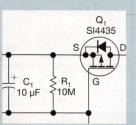*by Jay Esfandyari, Gang Xu, and Paolo Bendiscioli, STMicroelectronics*

COVER IMAGE: THINKSTOCK

Advanced power switches boost microhybrid emissions gains

27 Packaging and circuit integration deliver improved performance for start-stop automotive applications.

by Masashi Sekine and Jifeng Qin, International Rectifier Corp

DESIGN IDEAS

contents July 2012

pulse

Dilbert 14

DEPARTMENTS & COLUMNS

54

58

[www.edn.com]

EDN online

JOIN THE CONVERSATION
Comments, thoughts, and opinions shared by *EDN's* community

In response to "A virtual analog computer for your desktop," a technical article by Arthur Glazar at www.edn.com/4376400, antolin.agatep_#3 comments:

$$R\frac{di}{dt} + L\frac{d^2i}{dt^2} + \frac{i}{C} = \frac{dV}{dt}$$

"The point is not about tools, but in the methodologies that are being presented; that is, analog computers were used in solving for 'analytical' solutions to differential equations, which required the 'programmer' to understand the phenomena in differential or Laplace transform representation. Over many years ... the analog computer approach has fallen into disuse. But its foundations are solid and do rival the digital computer approach.

"Think of operational amplifiers when you think of analog computers. That's one of their most popular uses. But I have to say, as I've also studied analog circuits and design, that this methodology is far from dead."

In response to "Hearing aids hacked," posted in the Serious Fun blog at www.edn.com/4376762, AlisonKeen comments:

"I think there is merit in what these hackers are talking about. As someone who's worn hearing aids for a long time, it is frustrating to talk an audiologist through endless small adjustments that could be done at home ... [via] appropriately set-up software with appropriate hard-code limits.

"To put it into perspective, imagine if you could hook your glasses up to the computer and adjust the focus using some software. The excitement of being able to tinker and make the world clearer is a good incentive for something like this.

"Connecting in to your hearing aids is a good thing. ... If you have to wear the things, why not get the most out of them?"

EDN *invites all of its readers to constructively and creatively comment on our content. You'll find the opportunity to do so at the bottom of each article and blog post.*

CONTENT
Can't-miss content on EDN.com

DISCLESS CONSOLE GAMING: THE TIMES THEY ARE A-CHANGIN'

With the trend toward cloud-based processing and/or downloadable delivery and away from physical media for gaming already in play, recent moves by Sony have one engineer curious about its PlayStation design strategy.
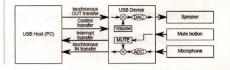
www.edn.com/4375555

FUNDAMENTALS OF USB AUDIO

Take a look at the USB Audio standard for digital audio and how it works, what to watch out for, and how to use USB Audio for high-fidelity multichannel input and output.

www.edn.com/4376143

ENGINEERING COMMUNITY
Opportunities to get involved and show your smarts

WHAT'S YOUR FAVORITE JOKE ABOUT ENGINEERS?

Who says engineers don't have a sense of humor? In late June, *EDN* asked its audience for their favorite joke about engineers or engineering. Nearly 100 jokes and comments have been posted so far, each one providing a good laugh. Check them out, and share your own, at **www.edn.com/4375942**.

EDN

BY PATRICK MANNION, BRAND DIRECTOR

Lasting impact of good engineering

had a nasty accident earlier this month that totaled my car but spared me and my passenger: my 11-year-old son, who was in the rear seat reading a book when we crashed. Everyone's OK, and the insurance companies will do their necessaries, but how do you mourn a great piece of engineering and thank the people behind it?

The crash was a split-second event. I had been driving along doing 45 to 50 mph when, out of nowhere, a red SUV appeared in front of me, its driver attempting a U-turn to go in my direction. I had nowhere to go; both lanes were blocked. Stopping was the only option. Screech, bang, smoke, fumes, fear, curb, witnesses, police, ambulance, neck braces, stretchers, and suddenly my son and I were lying side by side, blinkered and staring at the ceiling of an ambulance. I tried to reach my wife on a cell phone that, predictably, didn't work when I most needed it. My son clenched the Harry Potter book he'd been reading for the third time.

Eyewitnesses to the accident said I was "lucky" to have been able to slow down the car before impact; I credit the car's braking and good tires.

That book became a source of both comfort and humor at the scene. It was all my son wanted, and whenever someone tried to take it from him to make him lie down or examine him, he wouldn't let it go. In the end, he had to surrender it; but in the ambulance he reached up with both hands to take it from the officer who was handing it back to him, and he clutched it to his chest like a priest cradling the Gospels. I'll never shake that image.

They say you can tell a lot by what a person holds dear. So what does it say about me that, even as I counted my blessings, I felt a pang of grief when we arrived home later that evening and I saw the chasm where my car used to be?

I'm generally not too attached to things, but everyone knows I liked that car. It was a 2002 Maxima SE that I'd bought new with a view toward keeping it until its last gasp. I chose it because it had a good engine. Nissan had been hell-bent on making a name for itself

in quality, and '02 was the last year of that model, so all the bugs had long been worked out.

Ten years and 124,000 miles later, not a single part on that car had failed. Every button was intact; every moving part worked on cue. There had been no wiring problems, no engine trouble, and no sensor issues. I knew that every time I turned the ignition, the engine would start. The Nissan was reliable, trustworthy, and well engineered. It was the perfect car, serving me well even unto its demise.

Eyewitnesses to the accident said I was "lucky" to have been able to slow down the car before impact; I credit the car's braking and good tires. The crash nearly flipped the SUV, but the Nissan's front took the hit as designed: The airbags deployed, and the crumple zone sacrificed itself.

Meanwhile, we have a fridge—one of those Kenmore stainless-steel behemoths—that we bought new about

five years ago. Every year, we have to call Sears to fix the same water line. We know the repair guy by name.

My colleague Rich Nass recently complained about his own fridge heater breaking. "Who puts a heater in a freezer?" he exclaimed. It's just one more thing to fail.

I'm happy we came away relatively unscathed. I'm going to miss my car, though—not just because it was my car, but because it was one of the best examples of solid engineering I've had the pleasure to own.

Hats off to Nissan and to the engineers and designers who made that car. Thank you for keeping my son and me intact. EDN

Contact me at patrick.mannion@ubm.com.
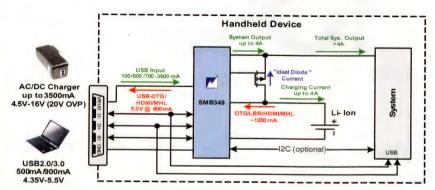
JOIN THE CONVERSATION

Any recommendations for a solid, utility car with a bit of oomph? Should I buy a used car or a new one? To comment, go to **www.edn.com/4389916**.

Finally! Charge Big Batteries Fast With 4A Chip-Scale Li-Ion Charger ICs

Flexible USB/AC Input from +3.6V to +16V, Tiny Solution Size, I²C Programmable Parameters and Built-In Safety – Ideal for Tablets and Smartphones
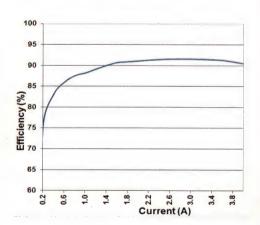
Applications
- Tablets
- Smartphones
- E-Readers
- UltraBooks
- Battery "JuicePacks"
- Portable Gaming
- Portable Digital Video

Features
- +3.6V to +16V Operating Input (+20V OV Protection)
- Fast-Charging, Flexible 4A Switch-Mode Architecture
  - *TurboCharge™** current-multiplier cuts charge time by 30%-60%
  - *TurboCharge+™** auto-float voltage control (AFVC) further reduces charge time by compensating for internal battery impedances
  - *CurrentPath™* with dual outputs for system/battery (SMB349) supports instant-on with dead/missing battery
  - *FlexCharge/FlexCharge+™** auto power source detection (APSD/AIVD) per USB2.0/3.0/BC1.2 to detect USB or AC/DC source +5V to +16V
  - *OptiCharge™** auto input current limit (AICL) detects and adapts to source current limit to maximize available power
- I²C Programmable Parameters and Functions with NV Configuration
- *SafeCharge™* safety features support JEITA/IEEE1725
  - Battery and IC over-voltage/current/temperature protection
  - Trickle charge for deeply-discharged cells
  - Safety timers and fault monitors/reporting
- Tiny 3.2 x 3.0 CSP and 52mm²/1.2mm z-height solution size

Industry's Highest System Efficiency

	SMB349	SMB359	SMB347	SMB137C	SMB346	SMB136C
Input Voltage Range (V)*	4.35 to 16 (20)	4.35 to 16 (20)	4.35 to 6.2 (20)	4.35 to 6.0 (18)	4.35 to 6.2 (20)	4.35 to 6.0 (18)
# of Inputs/Outputs	1/2	1/1	2/2	2/2	2/2	1/2
Maximum Charge Current (mA)	4000	4000	2500	1500	1250	1500
Maximum Input Current (mA)	3500	3500	2500	1500	2500	1500
CurrentPath™ Control	√		√	√	√	√
Charge Current Voltage Output	√	√	√		√	
Low-Battery Recovery Mode				√		√
Automatic Power Source Detection **	rev 1.2	rev 1.2	rev 1.1/1.2	rev 1.2	rev 1.1/1.2	rev 1.2
Package	3.2x3.0 CSP-49 5x5 QFN-40	3.2x3.0 CSP-49 5x5 QFN-40	3.0x2.5 CSP-30	3.0x2.5 CSP-30	3.0x2.5 CSP-30	3.0x2.5 CSP-30
Solution Size (mm2)	52	52	32	38	32	35

All chargers have Battery Thermal Protection & JEITA Support, IC Thermal Protection, Auto Input Current Limit, Safety or Watchdog Timers, Programmable Charging Parameters, I2C Interface, USB On-The-Go, TurboCharge™ Mode*

* Patent granted or pending

For more information see:
www.summitmicro.com/SMB349

SUMMIT
MICROELECTRONICS

Programmable Power for a Green Planet ™

pulse

INNOVATIONS & INNOVATORS

Scope enhancements simplify serial-bus debugging

As serial-bus standards have become faster and more complex, debugging has become a productivity issue. Firmware and software updates for several Tektronix digital and mixed-signal oscilloscope families reduce both serial-bus-test complexity and debug time, addressing such standards as PCIe, CAN/LIN, MIL-STD-1553B, and Media Oriented System Transport.

As signal complexity rises—for example, as multilane serial buses become commonplace—capturing unique events with an oscilloscope requires increasingly flexible trigger systems. Tektronix Visual Trigger lets you use a mouse or touchscreen to create highly customizable shapes that closely match the waveform of interest. A "mark all trigger events" feature enables search and capture of an acquisition's complex behaviors. For greater analysis depth, a custom interface to Matlab data-analysis software provides advanced plotting and filter capabilities. You can install and run Matlab on the scopes, thereby eliminating the need to transmit raw data to a separate computer for analysis.

Concern about crosstalk is rising along with bus speeds. The software helps Tektronix-oscilloscope users identify crosstalk in their designs without resorting to bit-error-rate testing. An algorithm in the DPOjet jitter- and eye-diagram-analysis tool correctly identifies crosstalk-induced jitter as bounded uncorrelated jitter; thus you can use real-time oscilloscopes to measure total jitter and separate crosstalk or intersignal interference from other forms of jitter. Using Microsoft Visual Studio, you can customize DPOjet measurements.

The new version of DPOjet is available now. Firmware updates for DPO (digital-phosphor oscilloscope)/MSO (mixed-signal oscilloscope) 5000 series, DPO7000C, and DPO/DSA (digital signal analyzer)/MSO70000C/D series oscilloscopes are available free at the Tektronix Web site. Before they can accept the updated firmware, however, many older instruments require Windows 7 installation, for which you must return the instrument to Tektronix. In the United States, the minimum charge for that is $692; the exact cost depends on what hardware must be replaced.

—by Dan Strassberg
▷**Tektronix Inc**,
www.tektronix.com.

You can now upgrade scopes in Tektronix's 5000, 7000, and 70000 series with firmware that greatly improves their serial-bus debugging capabilities. For owners of newer instruments—those that are already running Windows 7—the upgrade is free, requiring only a download and installation.

pulse

Multicore evaluation modules jump-start designs on TMS320C665x KeyStone-based DSPs

Texas Instruments is now offering two new EVMs (evaluation modules) for its KeyStone-based TMS320C665x multicore digital signal processors. The TMDSEVM6657L and TMDSEVM6657LE EVMs allow developers to get a quick start designing with the newest TI processors: the TMS320C6654, the TMS320C6655, and the TMS320C6657.

Combining fixed- and floating-point capabilities, TI's C665x multicore processors deliver real-time high performance at low power coupled with smaller form factors so that developers can meet the requirements of markets such as mission-critical systems,

industrial automation, testers, embedded vision, imaging, video surveillance, medical equipment, and audio and video infrastructure.

The TMDSEVM6657L EVM sells for $349, and the TMDSEVM6657LE sells for $549. Both modules include a free multicore software development kit, the company's Code Composer Studio integrated development environment, and a suite of

application/demo codes. The TMDSEVM6657L includes an embedded XDS100 emulator; the TMDSEVM6657LE includes a faster emulator, the XDS560V2, for quicker program load and ease of use.

Starting at just under $30 (10,000), the C665x processors offer developers access to devices that are high-performance as well as power-

The TMDSEVM6657L and TMDSEVM6657LE multicore processors from Texas Instruments include a free multicore software development kit, the company's Code Composer Studio integrated development environment, and a suite of application/demo codes.

and space-efficient. The low power consumption and 21×21-mm form factor enable portability, mobility, and low-power energy sources such as battery and interface powering to drive breakthrough products.

The C6657 features two 1.25-GHz DSP cores, delivering up to 80 GMACs and 40 Gflops; the C6655 and C6654 single-core solutions deliver up to 40 GMACs and 20 Gflops and 27.2 GMACs and 13.6 Gflops, respectively. Under normal operating conditions, the C6657, C6655, and C6654 power numbers are at 3.5, 2.5, and 2W, respectively.

—by Toni McConnel
Texas Instruments,
www.ti.com.

Microcontrollers target budget applications

The 32-bit STM32 F0 microcontrollers from STMicroelectronics use an ARM Cortex-M0 processor architecture, which lets developers break the price and performance limitations of older, 8- and 16-bit devices.

Built-in RAM-parity checking improves real-time performance and helps achieve Class B safety-standards compatibility in home appliances. An

integrated clock-security system enhances reliability, and advanced timing helps overcome common motor-control design challenges. The MCU integrates hardware touch-sensing control, a 12-bit ADC with 1M-sample/sec conversion, a 12-bit DAC, and two tightly coupled programmable analog comparators. A consumer-electronics control module allows connections to

home multimedia devices using industry-standard protocols.
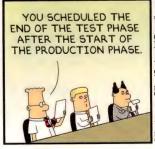
The MCU has a 1 5.3-µA stop mode and a 2.8-µA standby mode with the real-time clock running, extending battery life. Other features include an SPI with support for a programmable date frame as large as 16 bits and a baud rate as high as 18 Mbps, and an I²C port supporting communication speeds up to 1 Mbps.

The STM32 F0 offers embedded-memory densities of 16 to 64 kbytes of flash and 4 to 8 kbytes of SRAM, along with UFQFPN32, LQFP48, and LQFP64 package options. Another 20-pin version in 16-kbyte flash configuration and extension to 128-kbyte flash in a 100-pin package will soon become available. Programmable analog- and digital-noise filtering ensures robust communications, and a 6-Mbps USART supports multiple clock-input options.

A developer kit, including a prototype board, plugs directly into a PC's USB port; demonstration code and sample firmware support the kit. The kit sells for $7.99; the STM32 F0 sells for 95 cents (1000).

—by Fran Granville
STMicroelectronics,
www.st.com.

DILBERT By Scott Adams

YOU SCHEDULED THE END OF THE TEST PHASE AFTER THE START OF THE PRODUCTION PHASE.

WE'RE FEELING CONFIDENT.

IT'S TOO BAD THAT BEING SMART DOESN'T COME WITH SOME SORT OF GOOD FEELING LIKE THAT.

Rarely Asked Questions

Strange stories from the call logs of Analog Devices

Dual Op Amps and Double Agents: They may not always appear to be who they say they are…

Q: Are dual op amps just duplicates of the single version of the op amp? Do they offer the same performance?

A: That's a great question. Actually, there's quite a bit to it, from the perspectives of both the user and the IC designer. Multiple op amps (duals, triples, quads, and even the occasional octal) are very popular with customers who use many op amps in their circuits, and for good reason. Multiple op amps offer the advantages of less board area, reduced cost, and better matching. As for electrical performance, this cuts both ways, and we'll talk about it in a minute.

In many cases, multiple op amps are a very close approximation to the single amplifier. As you can imagine, there must be some redundancy the IC designer can take advantage of with two "duplicate" amplifiers, right? Yes, you're right; one example is the op amp's bias circuitry. Instead of duplicating the bias circuit for each op amp, it is often modified to accommodate all amplifiers, reducing complexity, die area, and cost. Reduced die area has a direct impact on the size and cost of the packaged op amps; it also lowers board cost (smaller board), assembly cost (one insertion), and inventory cost (one part vs. many). The amplifiers share a common piece of silicon, so they track extremely well, providing another advantage.

There are a few things to watch out for, however. Multiple op amps dissipate more power per package. Since the supply current is multiplied by the number of op amps, the power dissipation will increase; this can result in higher junction temperatures. As alluded to, multiples present challenges to the silicon designer as well. One of the issues with multiples is the layout. Compromises must be made, which can result in degradation in some electrical performance. Optimized for flow, size, and performance, the die layout can affect parameters such as offset voltage and drift. Also, due to tighter quarters, crosstalk can become an issue, especially at high frequencies. A few of ADI's high-speed amplifiers and differential amplifiers are offered with two separate die in a single package, however, providing excellent crosstalk performance and additional design freedom.

In summary, multiple op amps are a great choice when a circuit calls for several op amps, and for good reason: lower costs, smaller PCB area, easier inventory management, and better electrical performance.

Contributing Writer John Ardizzoni is a Technical Product Manager at Analog Devices in the High Speed Linear group. John joined Analog Devices in 2002, he received his BSEE from Merrimack College in N. Andover, MA and has over 30 years experience in the electronics industry.

Have a question involving a perplexing or unusual analog problem? Submit your question to: www.analog.com/askjohn

For Analog Devices' Technical Support, Call 800-AnalogD

GaN-on-GaN breakthrough LED boosts MR16 performance

Despite the ever-improving light output from white LEDs, the current technology still has some fundamental limitations. The technology typically employs silicon-carbide or sapphire substrates; manufacturers grow GaN (gallium nitride) on the substrate to form the active, or light-emitting, region in a white LED. The use of two materials causes a crystal-lattice mismatch, resulting in imperfections in the LED that, in turn, reduce the amount of the light that the device can produce.

Start-up Soraa—whose cofounder, Shuji Nakamura, discovered P-type doping in GaN and is thus responsible for the development of blue, green, and white LEDs—has developed the technology to grow GaN crystals on a native-GaN substrate so that the active-GaN-region crystals grow with fewer imperfections and can accommodate higher power densities. According to the company, that process allows the LED to emit five to 10 times more light from the same crystal area.

The company's first product is not an LED but rather a complete LED MR16 lamp. Although politicians have focused on the demise of the incandescent A-lamp, Soraa argues that the MR16 has a wider range of markets and applications. Europe, for example, currently uses more than 1 billion approximately 2-in.-long, 35 to 50W MR16 halogen lights, which sell for approximately $12 each.

Soraa's first product is not an LED but rather a complete LED MR16 lamp.

Depending on the version, the 12V-ac product family's performance approaches that of generic 50W halogen lamps, including crisp shadows and a similar color-rendering index.

Cree certainly sees the importance of this market: Last year it introduced a new, smaller-sized LED array targeted specifically for use in MR16s. The challenge was to get enough LEDs into an array to re-create the intense point source of the tiny halogen lights, while still keeping the warm color characteristics.

Cree's MT-G array crams 12 LEDs into a 9.1-mm^2 package. Those arrays are an improvement, but they still can't replicate the point-source performance of halogen. Shadows aren't sharp, and the light focus is limited because of the large source area.

This area is where Soraa's GaN-on-GaN-enabled 12V-ac product family shines: Depending on the version, the product family's performance approaches that of generic 50W halogen lamps, including crisp shadows and similar CRI (color-rendering index). The lamps include integral drivers that operate with several combinations of transformers and dimmers.

The standard version is offered at either 2700K or 3000K and 80 CRI, and a high-CRI version is available at 95 CRI. To reach high color-rendering with deep red, this version uses a violet-pumped triphosphor for a closer match to the black body than can be achieved with conventional blue-pumped two-phosphor technology.

Soraa made its initial announcement at Strategies in Light in February and demonstrated its products with four different lamps in its MR16 family at LightFair in May. I'm still puzzled as to why Soraa isn't offering its LEDs in component form, but I'd never, ever bet against Shuji Nakamura.
—**by Margery Conner**
▶ **Soraa**, www.soraa.com.

Hibernate capability aids power management

Mentor Graphics recently announced the addition of hibernate mode to its flagship embedded Nucleus RTOS (real-time operating system) power-management framework. The Freescale i.MX family of multimedia processors is the first in a line of devices that the hibernate capability of the Nucleus power-management framework supports.

The importance of power management in today's embedded designs is growing as embedded devices perform more complex tasks with limits placed on power consumption. The Nucleus power-management framework with hibernate capability lets software engineers design power-aware applications that can change the system's operating point to standby or hibernate mode during periods of inactivity, thereby reducing power consumption to reduce heat dissipation, meet energy requirements, and extend battery life. The high-level APIs (application-programming interfaces) within the Nucleus power-management framework provide access to the processor's power-management features, such as DVFS (dynamic voltage and frequency scaling) and clock gating, with only a few lines of code to allow software developers to create power-optimized products.—by Steve Taranovich
▶ **Mentor Graphics**, www.mentor.com.

07.12

EDN

Now Enhanced & Interactive

EXPERT CONTENT | DESIGN CENTERS | TOOLS & LEARNING | COMMUNITY

You turn to us for the resources, ideas, & solutions you trust.
Now get even more with the new **EDN.com**.

UBM
Electronics

pulse

PWM controllers enable smaller, greener power adapters up to 40W

The new PrimAccurate iW1699 and iW1760 digital PWM (pulse-width modulation) controllers from iWatt Inc allow power-adapter designers to meet stringent emerging global energy regulations for ac/dc power adapters—which require them to consume less than 100 mW of standby power—while enabling a lower bill-of-materials cost and smaller overall adapter size.

The iW1699 and iW1760 digital PWM (pulse-width modulation) controllers from iWatt allow power-adapter designers to meet stringent global energy regulations for ac/dc power adapters at a lower cost and a smaller size.

The iW1699 is optimized for applications up to 12W, with ultralow standby power, of less than 30 mW, to address the needs of smartphone and media-tablet applications. The iW1760 is designed for applications requiring higher power, up to 40W, with less than 50 mW of standby power, including set-top boxes, home-networking devices, and a range of household appliances.

The iW1699 and iW1760 PWM controllers build on iWatt's iW1691 digital controller but enable lower standby power and added design flexibility. Both new parts use the company's patented PrimAccurate primary-side control, which uses proprietary digital algorithms to eliminate the need for a secondary side regulator and optical feedback isolator, thereby reducing the overall solution size and improving reliability. PrimAccurate technology enables accurate control of the output over a range of operating conditions and ensures tight load and line regulation, along with full protection from fault conditions, without costly additional components.

The iW1699 and iW1760 PWM controllers are available now in production quantities. They come in a standard, low-cost, eight-lead small-outline IC package. In sample volumes, the iW1699 and the iW1760 are available for 30 cents (1000).

—**by Toni McConnel**
▷ **iWatt**, www.iwatt.com

BY BONNIE BAKER

Isolation has come a long way, baby!

ndustrial-circuit-design engineers use galvanic-isolation techniques to address safety issues, legal regulations, and ground-plane problems. If you have galvanic isolation in your circuit, you can exchange information and power between two points while preventing actual current flow. Galvanic isolation offers two main benefits. First, it protects people and equipment from potentially dangerous current and voltage surges. Second, it prevents unintentional ground loops from interfering with signals from data links and other interconnections.

Analog input/output, instrumentation, motion control, and other sensor interfaces often use a single-channel, isolated signal chain. These isolation channels separate the sensor circuitry in the factory floor's harsh environment from the signal-processing stage in the noise-free control-room environment.

You can use analog isolation amplifiers, isolated power supplies, digital couplers, or optocouplers for your galvanic-isolation requirements. The isolation barriers for these isolator circuits are constructed using capacitive, magnetic, or optoelectric technologies.

The single-channel, isolated temperature-measurement circuit in **Figure 1** uses a capacitive-coupled analog isolation amplifier. In this circuit, an RTD (resistance-temperature detector) converts temperature into a resistive value. A 100-µA current source converts the RTD resistance value to a voltage. The INA114 instrumentation amplifier gains the RTD/100-µA voltage and cancels the RTD wire resistances, R_L. The gain from the instrumentation amplifier matches the input-voltage range of the isolation amplifier.

The precision isolation amplifier uses duty-cycle modulation to transmit the instrumentation amplifier's output signal across a capacitive isolation barrier. The isolation amplifier is able to achieve a maximum of 1500V of galvanic isolation. This isolation device has an input-signal bandwidth of approximately 50 kHz, with a minimum power-supply requirement of ±4V. It is packaged in a 28-pin PDIP or SOIC.

An alternative design uses ADCs (**Figure 2**, available with the online version of this article at www.edn.com/4376379). The ADS1247 ADC has two internal current sources, a PGA (programmable-gain amplifier), and a delta-sigma modulator. The current sources convert the RTD resistance to voltage and cancel the effects of the three wire resistances. The PGA boosts the RTD input signal, and the converter produces a digital output signal.

The ISO7241 and ISO7221 digital isolators transmit the analog-to-digital configuration and conversion results across the isolation barrier. The isolators in **Figure 2** use internal capacitive isolation-barrier techniques to transmit the digital signal across the barrier with eight- and 16-pin packages.

It is difficult to say which isolation strategy will fit your application. You can apply these analog or digital isolation strategies to any signals that require galvanic isolation in the circuit using a variety of sensors that measure such quantities as temperature, pressure, and current.

Isolation amplifiers may be a fit because of your interest in remaining in the analog domain. They do, however, have higher power-supply requirements. Alternatively, you may prefer digital isolators because your signal eventually will convert to the digital domain.**EDN**

REFERENCE

[1] Kugelstadt, Thomas, "Industrial data-acquisition interfaces with digital isolators," *Analog Applications Journal*, Texas Instruments, 3Q11, http://bit.ly/MQjbpq.

Bonnie Baker is a senior applications engineer at Texas Instruments and author of A Baker's Dozen: Real Analog Solutions for Digital Designers.
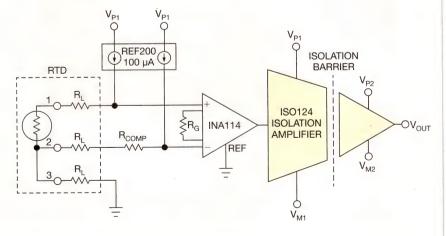
Figure 1 This single-channel, isolated temperature-sensor circuit uses a capacitive-coupled analog isolation amplifier.

Dissecting the Intel 710 Enterprise SSD
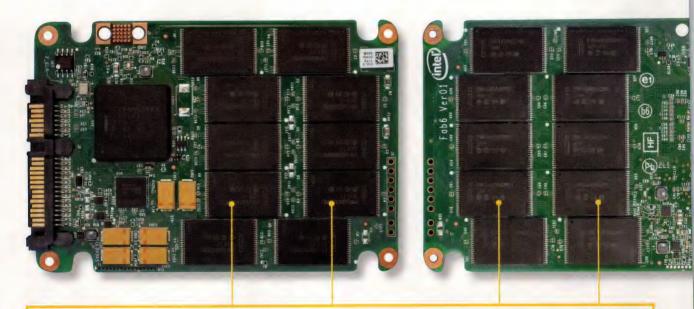
The main points of interest for Intel's 200-Gbyte 710 Enterprise SSD (solid-state drive) are that the design emphasis was mostly on endurance, reliability, and power efficiency. Also of note is the use of MLC (multilevel cell) NAND flash for primary storage. Intel refers to this implementation of MLC NAND in SSD design as HET (High Endurance Technology). According to Intel, HET comprises Intel-developed firmware, the Intel controller, and high-cycling NAND. The technology combines NAND silicon enhancements and unique SSD NAND management techniques to extend the write endurance of MLC-based SSDs for optimized endurance and performance. Intel HET firmware enhancements include optimized error-avoidance techniques, write-amplification reduction algorithms, and system-level error management beyond the normal industry ECC (error-correction code) standards.

SLC (single-level cell) flash is often the more desirable choice for enterprise SSDs, a consequence of the margin for error in reading a bit from a cell being very low while the endurance remains quite high. MLC flash, on the other hand, has occurrences of higher bit errors and suffers from the perception that it has much lower endurance. Efforts are being made, however, to use MLC flash in enterprise SSDs because they can provide more storage and reduce the cost of production.

Through HET implementation, Intel has thought of a way to attain MLC flash with higher reliability by exploiting the fact that not all MLC flash chips in a batch have the same characteristics. Some have higher read margins and improved retention quality than others, and an understanding of these characteristics is what makes up Intel's use of MLC NAND flash as HET in the Intel 710 SSD.
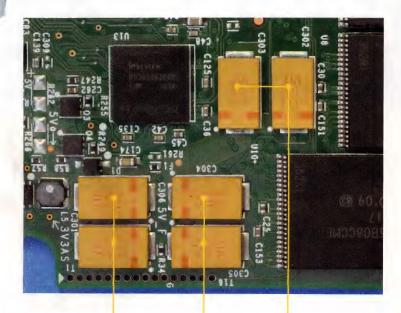
Twenty MT29F16B08CCME1 NAND MLC ICs, mirrored on the front and the back of the board, make up the storage of the 200-Gbyte version of the Intel 710. Each NAND flash device package contains two stacked 64-Gbit, 25-nm L74A NAND flash dice, making up 128 Gbits per package. The total flash capacity is actually 320 Gbytes, so a high level of overprovisioning was implemented.
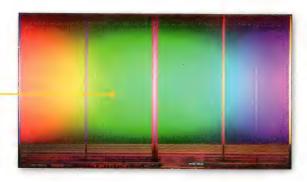
The controller uses a 512-Mbit Hynix H55S5162EFR mobile SDRAM for system memory. Intel's decision to utilize a mobile SDRAM makes sense, as it likely provides the required level of performance while, at the same time, minimizing power consumption. Reducing power consumption here is important because of the heavy amount of traffic that the DRAM would see while operating the drive, especially in enterprise applications.

Six 470-µF capacitors connected in parallel are used to store the required emergency charge and keep the drive alive long enough to flush out ongoing operations in the event of a power failure. Total capacitance is approximately 2.8 mF. This approach adequately powers the drive for a short amount of time without compromising large amounts of board space.

The SSD uses an Intel PC29AS21BA0 controller. Other Intel SSDs use this controller, but it is likely that a firmware update has made its operation unique to the 710 drive.

MECHATRONICS
IN DESIGN

FRESH IDEAS ON INTEGRATING
MECHANICAL SYSTEMS,
ELECTRONICS, CONTROL SYSTEMS,
AND SOFTWARE IN DESIGN

Engineering education upheaval

Information is a commodity; balancing and integrating information are not.

By Kevin C Craig, PhD

It is being talked about everywhere. "Harvard, MIT to Partner to Offer Free Online Courses," *The Boston Globe* heralded on May 3. "The Campus Tsunami," David Brooks of *The New York Times* proclaimed on the same day. Stanford University president John Hennessy, interviewed in the May 2012 *IEEE Spectrum*, foresees "the death of the lecture hall as university education moves online." The cover story of the summer 2012 ASEE *Prism* magazine reports a rekindling of the debate on the necessity of a master's degree for engineers; meanwhile, the ASEE has just released its 2012 report, "Innovation with Impact." It is clear that the industry warning "innovate or perish" applies to education as well, and it is time for action, not just talk.

I have heard it said that it is easier to move a cemetery than it is to change an engineering curriculum. Engineering schools for which that is true might soon be buried in those cemeteries. If information is a commodity—as I believe it now is—and if all engineering schools do is deliver traditional course content in a lecture format, then those schools will cease to exist, because that type of education has little impact on student learning and performance.

In engineering design, adding a sophisticated controller to a poorly designed physical system will never get it to offer outstanding performance. Similarly, traditional course content, even if the best lecturers in the world deliver it online, is still just information—a commodity. The problem is not the delivery method; the problem is the content of the delivery.

Engineering content must be rebundled and integrated with a balance between theory and industry best practices. Information thus becomes knowledge, which is not a commodity. Such knowledge stimulates students and transforms them into

critically thinking problem solvers, yielding a competitive advantage in the global economy.

Though the challenges for engineering education are being talked about everywhere, the only way to solve them is to change the culture, rejecting silos and comfort zones and instilling ownership. Until engineering education is viewed as an equal partner with engineering research in achieving innovation, that change will not happen.

A new concept for graduate-level education is emerging that could be applied to undergraduate education as well (**Figure 1**). It involves the creation of integrated, one-credit fundamental modules, delivered online. Such a structure works well for practicing engineers who must take courses part-time and who often find it easier to devote five weeks of intense effort to learning while working, instead of the typical 15 weeks of protracted study.

Once the modules have been completed, four three-credit online systems courses are taken that build on the modules. These stimulating, relevant, rewarding courses bridge fundamentals with actual practice. A six-credit onsite culminating experience completes the degree requirements.

The key is the integration and balance of theory with industry best practices. Such content does not exist in any one place; it must be gathered and integrated. Innovative industry leaders with passion will lead the way.

I am collaborating now with just such a leader to create a program in the area of fluid-power systems and control. Tom Price, president of Price Engineering, recognizes the value of this approach for his company, its workforce, his customers, and the United States. We need more industry leaders willing to step up and do the same.**EDN**
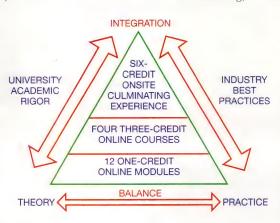
Figure 1 A new education concept comprises the creation of integrated one-credit fundamental modules, delivered online. The structure works well for practicing engineers who must take courses part-time and who often find it easier to devote five weeks of intense effort while working, instead of the typical 15 weeks of study.

ADVANCED POWER SWITCHES
BOOST MICROHYBRID EMISSIONS GAINS

PACKAGING AND CIRCUIT INTEGRATION DELIVER IMPROVED PERFORMANCE FOR START-STOP AUTOMOTIVE APPLICATIONS.

BY MASASHI SEKINE AND JIFENG QIN · INTERNATIONAL RECTIFIER CORP

Automotive start-stop operation, which reduces idling by shutting down a car's engine when the car momentarily stops, is a simple concept that can go a long way toward improving fuel economy and cutting emissions. The ICE (internal-combustion engine) system remained the predominant technology for vehicle propulsion among the roughly 80 million cars produced worldwide in 2011. Global trends, however, are conspiring to shift the balance toward alternatives. On one hand, the price of gasoline has skyrocketed; on the other, legislation governing emission standards is becoming more stringent worldwide.

In Europe, vehicle carbon-dioxide emissions are subject to a voluntary agreement between the European Union and automakers, but legislation has been pushed because overall performance remains way off the voluntary goal. Meanwhile, the Euro 6 standard, which requires substantial reductions in oxides of nitrogen emissions, will be phased in over the next few years. These developments ratchet up the challenges confronting automakers as they work to conform to evolving standards.

Clearly, reducing fuel consumption is one key to meeting the stringent new requirements. Toward that end, the market will boom in the next 10 years for HEVs (hybrid-electric vehicles) of all configurations—micro, mild, full, and plug-in—as well as for full EVs. Adoption of HEVs and EVs will be critical for meeting carbon-dioxide emissions targets for 2020.

AT A GLANCE

☑ Stopping the internal-combustion engine when a vehicle is not moving is a cost-effective method of cutting fuel use and emissions.

☑ Start-stop can be accomplished with dual batteries or with a battery and boost converter that stores energy in an inductor.

☑ Specialized battery power switches are available that disconnect the starter and main battery from the auxiliary electrical systems during engine start.

Research firm Yole Développement predicts that combined HEV/EV demand will increase this decade at a compound annual rate of 31% to reach 50 million cars in 2020, or about 50% of all cars produced that year (**Figure 1**).

Analysts expect microhybrid vehicles to account for most of that volume.

HYBRID TYPES

The major difference between micro-hybrid systems and full- or plug-in-hybrid systems is that microhybrids lack an electric powertrain to propel the vehicle. Rather, the microhybrid's start-stop system shuts down and restarts the ICE to reduce the amount of time the engine spends idling, such as when a car is sitting at a traffic light or in a traffic jam. The mild hybrid has a regenerative braking system in addition to the start-stop feature. Fuel-economy gains from these technologies are typically in the range of 5% to 10% compared with conventional vehicles' fuel-economy numbers (**Table 1**).

Various start-stop systems are available. One is the super starter, which uses a rugged dc starter plus a battery-management system. With a low, $80 average cost to the end user, super starters hold an estimated two-thirds of the total market for start-stop systems. Car manufacturers adopting the technology include BMW.

Another start-stop system is the BAS (belt-driven alternator starter), featuring a dc-ac inverter with average power typically in the 1.5- to 3-kW range. Such systems are virtually silent and offer an engine-restart time as low as 400 msec. With an estimated end-user price of approximately $300, BAS systems are found in many midpriced vehicles.

Finally, for conditions of extreme cold that can compromise the operation of conventional start-stop systems, a dual-battery solution or a dc-dc boost solution can be used to maintain the bus voltage.

TWO BATTERIES

In a typical dual-battery technology, when the ICE is running, power switch Q_1 remains on so that the load
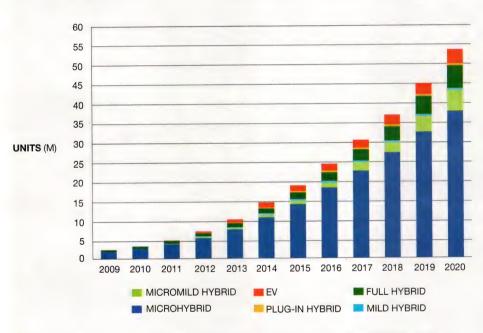
Figure 1 HEV/EV demand is forecast to increase 31% annually through 2020 (courtesy Yole Développement, August 2011).

TABLE 1 HEV TYPES BY FUNCTION

Function	Microhybrid/ micromild hybrid	Full hybrid	Plug-in hybrid
Start-stop	Yes	Yes	Yes
Regenerative braking	Yes (micromild only)	Yes	Yes
Electric drive	No	Yes	Yes
Recharge on grid	No	No	Yes
Fuel savings (%)	5 to 10	25 to 40	50 to 100

[www.edn.com]

is fully supplied by the main battery as well as an alternator (**Figure 2**). When the vehicle stops, the ICE turns off, and the main battery becomes the only source of power supply to the load. At engine restart, the main-battery voltage must supply a transient current as high as 1000A to the starter motor, resulting in a transient-voltage drop at the main-battery terminal to as low as 6V.

To prevent the power-electronics circuit from shutting down due to the battery-cranking transient event, a controller sends a turnoff signal to Q_1 to disconnect the main battery from the load. The auxiliary battery then supplies power to the load and maintains the battery voltage. After the engine restarts successfully and the alternator resumes operation, Q_1 is turned on and the system reenters vehicle running mode.

Power switch Q_1 and the controller are also used as a part of a reverse battery-protection circuit. If the main battery is connected in reverse polarity, Q_1 stays off because no signal is coming from the controller. It protects circuitry on the load by terminating the reverse-current-flow path.

DC-DC BOOST

A similar configuration uses a dc-dc boost converter instead of an auxiliary battery (**Figure 3**). At engine restart, bypass switch Q_1 disconnects the main battery from the load, and a dc-dc converter supplies a boosted voltage to the load during the cranking period.

The dc-dc boost converter comprises one inductor, two power switches (Q_2 and Q_3), and one output capacitor. All energy is stored at the inductor when Q_2 turns on. Q_3 would be off at that time. The inductor then transfers the energy to the load through Q_3 when Q_2 is off. The voltage on the main battery and the voltage on the load terminal determine the duty cycle of Q_2. A PWM controller operates this type of synchronous dc-dc boost converter in continuous-conduction mode to maintain the voltage on the load terminal.

MICROHYBRID EXAMPLE

For the battery switch, International Rectifier's AUIRF1324S-7P surface-mount MOSFET delivers a maximum on-state resistance as low as 1 mΩ and an output current up to 240A. For through-hole packaging requirements, the company offers the AUIRF1324L in a conventional TO-262 with a maximum on-state resistance of 1.65 mΩ.

The wide-lead, TO-262-packaged AUIRF1324WL power MOSFET can reduce the maximum on-state resistance by roughly 20%. Wider-lead packages mean more areas fit the internal wirebonds at the MOSFET's source terminal. The lower on-state resistance and the improved wirebonding inside the package collectively yield an approximately 30% increase in the maximum-drain-current rating.

All MOSFETs in the 24V 1324 family are suitable candidates for battery-switch applications. IR also offers 40V automotive-grade MOSFETs with an on-state resistance as low as 1.25 mΩ. These products are suited for dc-dc-converter applications.

The AUIR3240S, an automotive-grade high-side MOSFET driver, drives
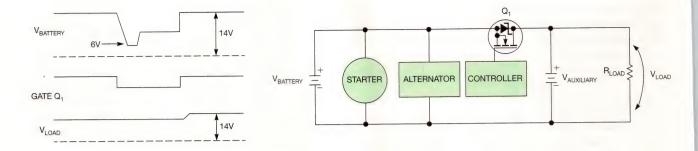
Figure 2 Dual-battery switch technology in the microhybrid system uses an auxiliary battery to provide high starting currents for start-stop operations. During start, Q_1 disconnects the main battery from the power-electronics circuit, to which the auxiliary battery then supplies the correct voltage.
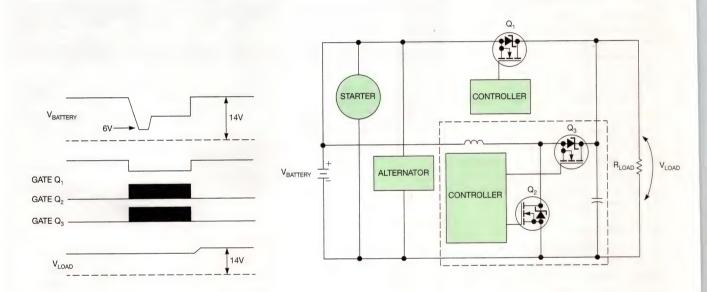
Figure 3 The dc-dc boost converter topology in a microhybrid system stores energy in the converter inductor. Here the boost converter (dotted box) functions as the auxiliary battery in the dual-battery system.
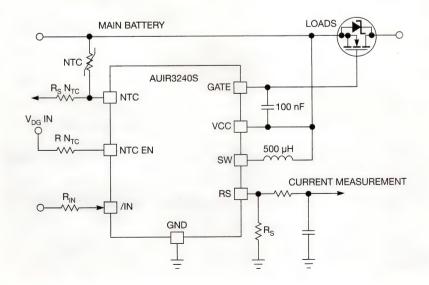
Figure 4 The dual-battery system can use the board-net stabilizer in the highly integrated AUIR3240S power-switch high-side MOSFET driver. The power switch disconnects the starter and battery from auxiliary systems when the engine is started.

the battery power switch for start-stop applications (**Figure 4**). The highly integrated boost converter was designed specifically for start-stop systems, which require a board-net stabilizer that uses a power switch to disconnect the starter and main battery from the auxiliary electrical systems during engine start. The AUIR3240S can drive several MOSFETs in parallel to achieve very low on-state resistance, with current consumption of less than 50 µA. The device provides 15V on the output, with a wide input voltage of 4 to 36V. The AUIR3240S also features diagnostics on the output current and a thermal sensor interface for a robust design.

Continued development of micro-hybrid start-stop systems requires solutions for reducing the cranking voltage drop, integrating more electronics into the starter and furthering the evolution of battery technologies. Power-electronics vendors and automakers are putting the components in place to make the necessary advancements.**EDN**

ACKNOWLEDGMENT

AUTHORS' BIOGRAPHIES
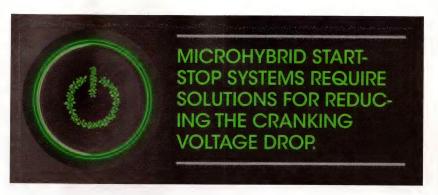
Masashi Sekine is an applications and technical marketing engineer in the Automotive Product business unit of International Rectifier (El Segundo, CA). He supports field activities related to MOS-FET-based automotive applications as well as product specifications and definitions. Sekine holds a bachelor of science degree in electrical engineering from Tokyo Institute of Technology and has 10 years of experience in power electronics.
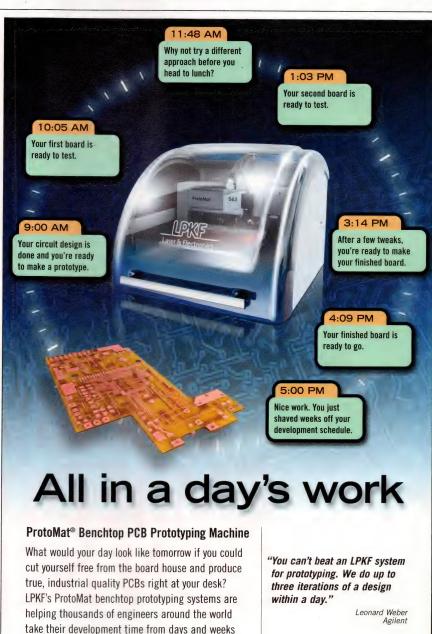
Jifeng Qin is a product manager in the Automotive Product business unit of International Rectifier. He holds a bachelor of science degree in electrical engineering from Zhejiang University (Hangzhou, Zhejiang, China) and a master's degree in electrical engineering from North Carolina State University. Qin has more than five years of experience in circuit design, application, and marketing, and he holds seven US patents.
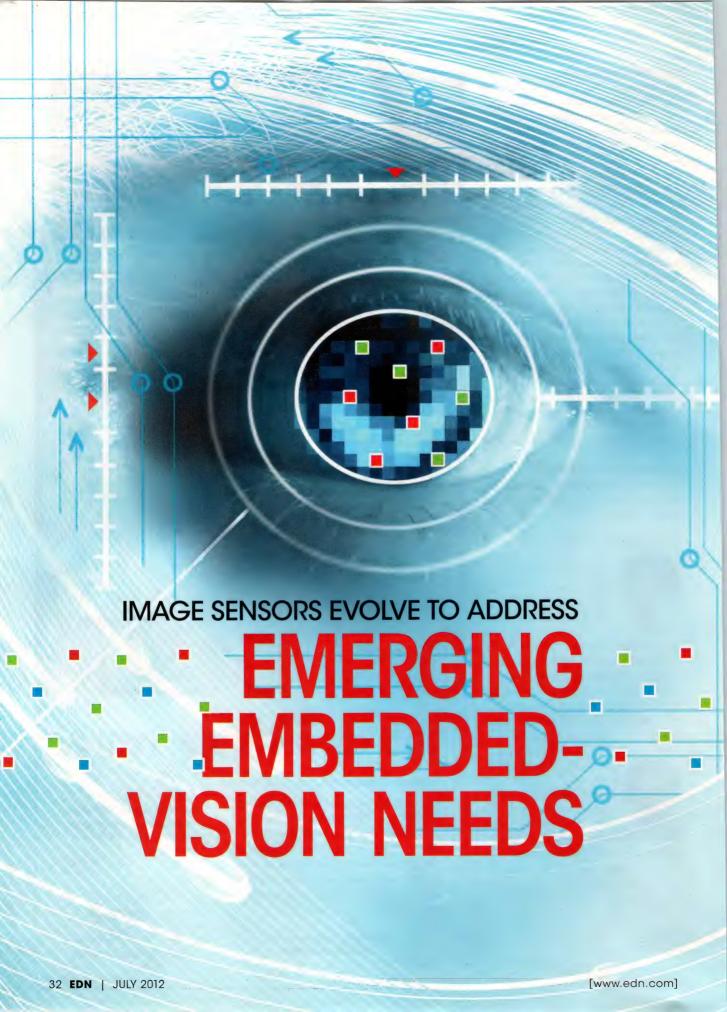
IMAGE SENSORS EVOLVE TO ADDRESS

EMERGING EMBEDDED- VISION NEEDS

AS TECHNOLOGY PROGRESSES FROM ELEMENTARY IMAGE CAPTURE TO MORE ROBUST IMAGE ANALYSIS, INTERPRETATION, AND RESPONSE, SEMICONDUCTOR SUPPLIERS AND THEIR OPTICS PARTNERS ARE RESPONDING WITH IMPROVED IMAGE-SENSOR SUBSYSTEMS.

BY BRIAN DIPERT · EMBEDDED VISION ALLIANCE, AND ERIC GREGORI AND SHEHRZAD QURESHI · BDTI

L ook at the systems you're designing, or more generally at the devices that surround your life, and you're likely to see a camera—or a few—staring back at you. Image sensors and their paired image processors are an increasingly common presence in a diversity of electronic products.

It's nearly impossible to purchase a laptop computer without a bezel-mount camera, for example, and a rising percentage of all-in-one desktop PCs, dedicated computer displays, and even televisions now include them as well. Smartphones and tablets, too, frequently feature image sensors, often located on both the front *and* back panels, and sometimes even arranged in "stereo" configurations for 3-D image capture. You'll even find cameras embedded in portable multimedia players and mounted in cars.

IMAGE(S): THINKSTOCK

APPLICATION ABUNDANCE

The fundamental justification for including a camera in a design is often to enable elementary image capture, notably for still photography, videography, and videoconferencing. Given that the imaging building blocks are already in place, however, software and system developers are also leveraging them for more evolved purposes, such as discerning meaning from the content and taking appropriate action in response to the interpreted information.

In the vehicle use case, for example, an advanced analytics system doesn't just "dumbly" display the rearview camera's captured video feed on an LCD but also warns the driver when it detects an object behind the vehicle. Advanced implementations might go so far as to slam on the brakes to preclude impact.

Additional cameras, mounted both inside the vehicle and in various locations around it, alert the driver to—and, in advanced implementations, take active measures to avoid—unintended lane transitions and collisions with objects ahead. They can also discern road signs' meanings and consequently alert the driver to excessive speed or potentially dangerous roadway conditions. The cameras further can minimize driver distraction by enabling gesture-interface control of the radio and other vehicle subsystems, and they can snap a dozing, texting, or otherwise multitasking driver back to full attention to the road.

Smartphones, tablets, computers, and televisions employ front-mounted image sensors for diverse purposes. They can alert a user who is sitting too close to or too far away from the display, or whose posture is poor. They can ensure that the display backlight stays on as long as a person is positioned in front of the display, and, conversely, they can auto-power down the display when the person steps away. Gesture interfaces play an increasingly important role in these and other consumer-electronics

ONLINE EXCLUSIVE

Part 2 of this article, available exclusively online, discusses HDR processing for embedded vision. Read it at **www.edn.com/4375325**.

AT A GLANCE

↘ With the increased performance, decreased cost, and reduced power consumption of processors, image sensors, memories, and other semiconductor devices, developers are evaluating embedded-vision capabilities for a diversity of system form factors and price points.

↘ A conventional image-sensor-based design can support many embedded-vision implementations, but for depth-cognizant requirements, a 3-D image-sensor subsystem is often necessary.

↘ Common methods for depth mapping are stereo sensor arrays, which "bolt" together two cameras; structured light, which projects a predetermined light pattern onto a scene for analysis; and time of flight, which derives range from the time it takes for projected light to travel from the source to the object and back to the sensor.

applications, such as game consoles, supplementing—if not supplanting—such traditional mechanisms as button and key presses or trackpad or mouse swipes and clicks.

A forward-facing camera can monitor respiration, by measuring chest rise-and-fall cadence, and heart rate, by detecting the minute, cyclical variance in facial color caused by blood flow. It can monitor eyeball drift to warn a user who has had too much to drink. It can identify an authorized user who appears in front of a system, automatically logging in that person and loading account-specific programs and settings. A rear-mount camera, meanwhile, can employ augmented reality to supplement the conventional view of an object or scene with additional information.

These examples typify embedded vision, a burgeoning application category that extends to dedicated-function devices such as surveillance systems and manufacturing-line inspection equipment. In some cases, computers running PC operating systems historically handled the vision-analytics task, although such approaches were costly, bulky, high-power, and unreliable. In other situations, any or all of those same

factors made it inherently impractical to implement vision functionality.

Now, with the increased performance, decreased cost, and reduced power consumption of processors, image sensors, memories, and other semiconductor devices, developers are evaluating embedded-vision capabilities for a diversity of system form factors and price points. That activity has also prompted the need for increasingly robust imaging subsystems (see **sidebar** "Focus: the fourth dimension," available online at http://bit.ly/PPlwEe).

RANGE VERSUS RESOLUTION

For many years, a "more megapixels is better" mentality fueled the consumer digital-camera market, whose constituent image sensors—by virtue of their high volumes and consequently low prices—also find homes in many embedded-vision systems. In recent times, however, the limitations of such a simplistic selection strategy have become progressively more apparent.

For one thing, consumers increasingly realize that unless they're printing wall-sized enlargements or doing tight crops of a source photo, they don't need high-resolution images, which take up significantly more storage space than their lower-resolution precursors. For another, the noisy and otherwise artifact-filled images that modern cameras generate reveal the lithography-driven downside of the increasing-resolution trend.

Sensors must remain small in overall dimensions to remain cost-effective—a critical attribute in consumer-electronics systems. As manufacturers shoehorn an increasing number of pixels onto sensors, individual pixel dimensions must therefore predictably shrink. Smaller pixels collect fewer photons in a given amount of time, thereby leading to decreased light sensitivity. That phenomenon not only degrades a camera's low-light performance but also adversely affects the system's dynamic range. Postprocessing can only partially compensate for that compromise, and then often only with motion artifacts and other trade-offs (see **Part 2** of this article, "HDR processing for embedded vision," available online at www.edn.com/4375325).

Ironically, embedded-vision-focused applications tend to have lower resolu-

tion requirements than does general-purpose photography. The infrared- and visible-light image sensors in Microsoft Corp's Kinect, for example, are VGA (640×480-pixel) resolution models, and the vision peripheral passes only along QVGA (320×240-pixel) depth-map images to the connected game console or PC.

Given the plethora of available pixels in modern sensors, some suppliers leverage the surplus to improve both light sensitivity and color accuracy by migrating beyond the conventional Bayer RGB-pattern filter-array approach (**Figure 1**). Additional—and altered—filter colors are claimed to enhance full-spectrum per-pixel interpolation results, whereas monochrome, or filterless, pixels let in even more light, at the trade-off of dispensing with color discernment (**Reference 1**).

Leica Camera AG's latest digital still camera takes filter alteration to the extreme, capturing only black-and-white images by virtue of its filterless monochrome image sensor (**Figure 2a**). Reviewers, however, espouse the sharpness of the camera's photographs even at high ISO settings.

Meanwhile, Nokia Corp's 808 PureView smartphone embeds a 41M-pixel image sensor but by default outputs 8M-pixel or lower-resolution images (**Figure 2b** and **Reference 2**). By combining multiple pixels in variably sized clusters depending on the digital zoom setting, the 808 PureView dispenses with the need for a complex, costly, and bulky optical zoom structure and multiplies the effective per-image-pixel photon-collection capability for improved low-light performance.

Sony Corp has pioneered a sensor-design technique called backside illumination (**Figure 2c**). Implementation specifics aside, the technique routes the interpixel wiring behind the pixels' photodiodes to improve a sensor's per-pixel fill factor—the percentage of total area devoted to light collection—and therefore its low-light capabilities.

DEPTH DISCERNMENT

A conventional image-sensor-based design can support many embedded-vision implementations. It can, for example, assist in interpreting elementary gestures, as well as tackle rudimentary facial-detection and -recog-

nition tasks, and it is often adequate for optical-character-recognition functions. It might not, however, cleanly detect elaborate gestures that incorporate movement toward or away from the camera (3-D), as opposed to gestures strictly in the vertical and horizontal planes (2-D). More generally, it cannot fully discern the entirety—that is, the depth—of an object; for example, it cannot easily distinguish between a person's face and a photograph of that person. For such depth-cognizant requirements, a 3-D image-sensor subsystem is often necessary (**Reference 3**).

Regardless of the specific 3-D sensor implementation, the common output is the depth map, an image matrix in which each pixel-data entry—which is sometimes additionally color-coded for human-interpretation purposes—represents the distance between the sensor and a point in front of the sensor (**Figure 3**). Each depth-map frame commonly mates with a corresponding frame captured by a conventional 2-D image sensor, with the two frames parallax-corrected relative to each other because they source from

Figure 1 The Bayer sensor pattern, named after a Kodak imaging scientist, remains the predominant filter-array scheme used in digital imaging applications (a). More modern approaches increase the number of green-spectrum pixels in a random pattern for enhanced detail in this all-important portion of the visible-light spectrum (b), leverage subtractive colors—at the trade-off of greater required postprocessing—in order to improve the filters' light-transmission capabilities (c), and even add filterless monochrome pixels to the mix (d).

(a)

(b)

(c)

FRONT-ILLUMINATED STRUCTURE

BACK-ILLUMINATED STRUCTURE

ON-CHIP LENS
COLOR FILTER
METAL WIRING

PHOTO-DIODE SUBSTRATE

LIGHT-RECEIVING SURFACE
PHOTODIODE
SUBSTRATE

METAL WIRING

MICROLENSES
COLOR FILTERS

LENSES
RED   GREEN

INCIDENT LIGHT

ON-CHIP LENS
COLOR FILTER
SI SURFACE
BACK SIDE

METAL
INTERCONNECTS

M2
M1

PHOTODIODE

SI SUBSTRATE

PHOTOSENSITIVE
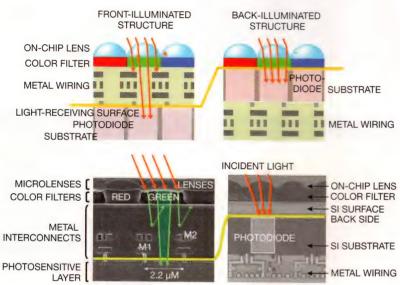LAYER

2.2 μM

METAL WIRING

Figure 2 Leica's M Monochrom will set you back $8000 or so and captures only black-and-white images, but reviewers rave about the camera's sharpness and low-light performance (a). The Nokia 808 PureView smartphone packs an enormous, 41M-pixel image sensor, which it uses to implement digital zoom and clustered-pixel photon-collection capabilities (b). A Sony-pioneered sensor-design technique called backside illumination routes the interpixel wiring behind the photodiodes, thereby improving the per-pixel fill-factor ratio (c).

separate cameras in separate locations.

One common method of discerning depth is by means of a stereo sensor array, which arranges two image sensors in a configuration reminiscent of a pair of eyes. As with the human brain and eyes, an imaging SOC processes the sensors' differing-perspective viewpoints of an object to assess the distance between the object and the sensor array. It's possible to extend the concept beyond two sensors in multiview-geometry applications. The dual-sensor approach is often the lowest-cost, lowest-power-consump-tion, smallest-form-factor option, and it's particularly attractive if the sensors are already present in the design for 3-D still-image photography and video capture.

One stereo-imaging implementation is the discrete "binocular" approach, achieved by "bolting" together two cameras. Although this version of the concept may be the most straightforward from a hardware standpoint, the required software support is more complex. By way of analogy, two motorcycles linked together with a common

(a)

(b)

(c)

(d)

Figure 3 Regardless of the specific 3-D camera technique employed, they all output a depth map of objects they discern (a). A device such as the HTC EVO 3-D smartphone, whose stereo sensor array is primarily intended to capture 3-D still and video images, can also be used for 3-D embedded-vision purposes (b). Microsoft's Kinect (c) harnesses the structured-light method of discerning depth by projecting a known infrared-light pattern in front of it and then analyzing the shape and orientation of the ellipses that it sees (d).

axle do not make a car. The cameras require calibration for robust image registration, and their frames must be synchronized if—as is commonly the case—either the camera array or the subject is moving.

Alternatively, it's possible to combine two image sensors in a unified SOC or multidie package, outputting a combined data stream over one bus. The advantages of the fully integrated approach include improved control and frame synchronization. The tighter integration improves calibration, which in turn yields better stereo-imaging results, manifested as increased depth perception and faster image processing.

PROJECTION APPROACHES

Structured light, the second common 3-D sensor scheme and the technology used in Microsoft's Kinect, projects a predetermined pattern of light onto a scene for the purpose of analysis. The structured-light method's 3-D sensor scheme uses a projector to create the light pattern and a camera to sense the result.

In the case of the Kinect, the projector employs infrared light. Kinect uses an astigmatic lens with different focal lengths in the x and y directions. An infrared laser behind the lens projects an image comprising a large number of dots that transform into ellipses, whose particular shape and orientation in each case depend on the object's distance from the lens.

Advantages of the structured-light approach include its finely detailed resolution and its high accuracy, notably in dimly illuminated environments where visible-light spectrum-focused image sensors might struggle to capture adequate images. Structured-light software algorithms are also comparatively simple compared with the stereo sensor approach, although the concomitant point-cloud processing can be computationally expensive, approaching that of stereo vision.

Conversely, the structured-light technique's reliance on infrared light, at least as manifested in the Kinect, means the technology will have issues operating outdoors, where ambient infrared illumination in sunlight will destructively interfere with the light coming from the projector. The projec-

tor is also costly and bulky, consumes substantial power, and generates a large amount of heat; indeed, Kinect contains a fan specifically for this reason (**Reference 4**). The necessary custom projector lens adds to the total bill-of-materials cost.

Time of flight is the third common method of implementing a 3-D sensor. As with structured light, a time-of-flight camera contains an image sensor, a lens, and an active illumination source. With time of flight, however, the camera derives range, or distance, from the time it takes for projected light to travel from the transmission source to the object and back to the image sensor (**Reference 5**). The illumination source is typically either a pulsed laser or a modulated beam, depending on the image-sensor type that the design uses.

Image sensors that integrate digital time counters typically combine with pulsed laser beams, as do shutter-inclusive range-gated sensors. In the latter case, the shutter opens and closes at the same rate with which the projector emits the pulsed beam. The amount of light each image-sensor pixel "sees" is therefore related to the distance the pulse traveled, hence the distance from the sensor to the object. Time-of-flight designs that include image sensors with phase detectors conversely use modulated-beam sources. The strength of the beam varies over time, and so measuring the incoming light's phase indirectly derives the time-of-flight distance.

Time-of-flight cameras are common in automotive applications, such as pedestrian detection and driver assistance, and are equally prevalent in robotics products. They also have a long and storied history in military, defense, and aerospace implementations. The required image-processing software tends to be simpler, and therefore more real-time-amenable, than the requisite software for stereo camera setups, although the time-of-flight technique's susceptibility to ambient-

illumination interference and multiple reflections somewhat complicates the algorithms.

Frame rates for time-of-flight approaches can be quite high—upward of 60 frames per second, a speed that's difficult to achieve with stereo imager setups—but the comparative resolution is usually lower. And, as with the structured-light technique, the required time-of-flight light projector translates into cost, power consumption (and heat dissipation), size, and weight downsides.

ALLIANCE, DESIGN SUCCESS

Embedded-vision technology has the potential to enable electronic products that are more intelligent and responsive, and thus more valuable to users, than ever before. The technology can add helpful features to existing products, and it can provide significant new markets for hardware, software, semiconductor, and systems manufacturers.

The Embedded Vision Alliance, a worldwide organization of technology developers and providers, was formed last summer to provide engineers with the tools necessary to speed the transformation of this potential into reality. The mission of the alliance is to provide practical education, information, and insights to help engineers incorporate embedded-vision capabilities into products (see **sidebar** "The Embedded Vision Alliance," available online at http://bit.ly/M0GxrI).**EDN**

REFERENCES

1 Embedded Vision Alliance, "Selecting and Designing with an Image Sensor: The Tradeoffs You'll Need to Master," http://bit.ly/LcEdRf.

2 Embedded Vision Alliance, "Nokia's 808 PureView: A Technical Article and Several Videos For You," March 5, 2012, http://bit.ly/LxiOln.

3 Embedded Vision Alliance, "March 2012 Embedded Vision Alliance Summit Technology Trends Presentation on Image Sensors," http://bit.ly/Nfctdn.

4 Ifixit, "Microsoft Kinect Teardown," http://bit.ly/LcEy6y.

5 Embedded Vision Alliance, "Time of Flight: Samsung's New RGB Image Sensor Also Has Depth Sight," March 1, 2012, http://bit.ly/N5abtU.

AUTHORS' BIOGRAPHIES

Brian Dipert is editor-in-chief of the Embedded Vision Alliance. He is also a senior analyst at BDTI, a source of analysis, advice, and engineering for embedded processing technology and applications, and editor-in-chief of InsideDSP, BDTI's online newsletter dedicated to digital-signal-processing technology. Dipert has a bachelor's degree in electrical engineering from Purdue University (West Lafayette, IN). He began his career at Magnavox Electronics Systems (Fort Wayne, IN), and subsequently spent eight years at Intel Corp (Folsom, CA) as well as 14 years at EDN.

Eric Gregori is a senior software engineer and embedded-vision specialist with BDTI. He is a robot enthusiast and has more than 17 years of embedded-firmware design experience. Gregori's specialties are computer vision; artificial intelligence; and programming for the Windows Embedded CE, Linux, and Android operating systems. He created the Robot Vision Toolkit and developed the RobotSee Interpreter. Gregori is working toward his master's degree in computer science. He holds 10 patents in industrial automation and control.

Shehrzad Qureshi is a senior engineer with BDTI and principal of Medallion Solutions LLC. He has a master's degree in computer engineering from Santa Clara University in California and a bachelor of science degree in computer science from the University of California, Davis. He is an inventor or co-inventor on eight US-issued patents and has more pending. Qureshi earlier in his career was director of software engineering and acting director of IT at Restoration Robotics; before that, he was the software manager at biotech start-up Labcyte. He has held individual-contributor positions at Accuray Oncology, where he worked in medical imaging, and Applied Signal Technology, where he worked on classified signals-intelligence defense programs. Qureshi is the author of Embedded Image Processing on the TMS320C6000 DSP (Springer, 2005).

BY JAY ESFANDYARI, GANG XU, AND PAOLO BENDISCIOLI · STMICROELECTRONICS

Applying the interrupt features of MEMS accelerometers

UNDERSTAND HOW TO IMPLEMENT RELIABLE AND ROBUST INTERRUPT-BASED APPLICATIONS USING MEMS-BASED ACCELEROMETERS.

Most of the latest three-axis digital micro-electromechanical-system accelerometers on the market can generate interrupts for a number of applications. Some of the applications, including screen rotation, wake-up, free-fall, and single- and double-click recognition, are popular, and designers have implemented them in various devices.

A digital MEMS accelerometer usually has one or two interrupt-output pins that can be interfaced with the I/O pins of an external host processor. You can configure the accelerometer to monitor acceleration or motion in the background or simply to stay in low-power, sleep mode while the host processor performs other tasks. When the accelerometer detects an interrupt, the host processor can then wake up to check whether the interrupt needs to be served.

DATA-READY INTERRUPT
You can configure a digital MEMS accelerometer to generate a signal to indicate when a new set of measurement data is available for reading. The data-ready bit in the status register of the accelerometer, which is accessible to users, usually represents this signal. You can route the signal to an inter-

rupt pin by enabling the data-ready interrupt bit in one of the control registers, and you can set its polarity to active-low or active-high through the edge-level bit in another control register. By default, the interrupt pin is active-high when the accelerometer powers up.

The data-ready interrupt signal goes high when a new set of acceleration data has been generated in the data registers of the accelerometer. The interrupt goes low when the system has read the high bytes of the data registers of all enabled axes. If the system has not read the high bytes during one output-data-rate period, then the data-ready interrupt will remain high, and the overrun bit in the status register becomes one. In this case, data overrun has occurred, and the system has overwritten the previous data samples.

You can use the data-ready interrupt feature to synchronize continuous data acquisition and prevent data loss. By default, the interrupt pin is a push-pull topology, which can be tied directly to a host-processor I/O port that has an interrupt function. When new data is not ready, the host processor can perform other tasks or simply stay in sleep mode.

Once the data-ready interrupt occurs, the host processor can wake up at the rising edge of the I/O port to enter the interrupt-service subroutine and then read and process the acceleration data. That action can help reduce the overall system power consumption because it relieves the host processor of the task of continuing to poll the data-ready bit in the status register. During accelerometer evaluation, you can use the data-ready interrupt to check the frequency of the interrupt signal's waveform at different output-data rates by using an oscilloscope.

FREE-FALL INTERRUPT
Accelerometer designers widely use the devices' free-fall interrupt feature in hard-disk-protection applications. When, for example, a laptop computer is falling, the laptop computer's embedded accelerometer can generate an interrupt so that the hard drive can park the magnetic head of the disk in a safe place to prevent mechanical damage to the disk.

Designers of medical systems can also integrate the accelerometer's free-fall interrupt with a MEMS

Figure 1 The accelerometer's evaluation board and its Windows demo software capture the device's raw data and the interrupt signal.

DESIGN NOTES

42V, 2.5A Synchronous Step-Down Regulator with 2.5µA Quiescent Current

Design Note 504

Hua (Walker) Bai

Introduction

The LT®8610 and LT8611 are 42V, 2.5A synchronous step-down regulators that meet the stringent high input voltage and low output voltage requirements of automotive, industrial and communications applications. To minimize external components and solution size, the top and bottom power switches are integrated in a synchronous regulator topology, including internal compensation. The regulator consumes only 2.5µA quiescent current from the input source even while regulating the output.

High Efficiency Synchonous Operation

Replacing an external Schottky diode with an internal synchronous power switch not only minimizes the solution size, but also increases efficiency and reduces power dissipation. The efficiency improvement is significant in low output voltage applications where the voltage drop of the Schottky diode represents a relatively large portion of the output voltage. Figure 1 shows a 12V to 3.3V circuit. Figure 2 shows the efficiency of this circuit reaching 94%, which is 5% to 10% higher than a comparable nonsynchronous circuit.

Short-Circuit Robustness Using Small Inductors

The LT8610 and LT8611 are specifically designed to minimize solution size by allowing inductor size to be selected based on the output load requirements of the application, rather than the maximum current limits of the IC. During overload or short-circuit conditions, the LT8610 and LT8611 safely tolerate operation with saturated inductors through the use of a high speed peak-current mode architecture and a robust switch design. For example, an application that requires a maximum of 1.5A should use an inductor that has an RMS rating of >1.5A and a saturation current rating of >1.9A. This flexibility allows the user to avoid oversize inductors for applications requiring less than maximum output current.

Current Sense and Monitoring with the LT8611

The LT8611 includes a flexible current control and monitor loop using the ISN, ISP, IMON and ICTRL pins. The ISP and ISN pins connect to an external sense resistor that may be in series with the input or output of the LT8611 or in series with other system currents. The current limit loop functions by limiting the LT8611 output current such that the voltage between the ISP
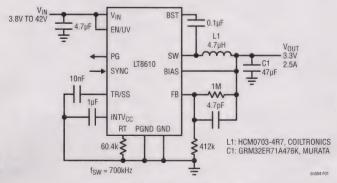
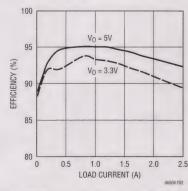**Figure 1. LT8610 12V to 3.3V Application Achieves High Efficiency**

Figure 2. Efficiency of the 12V to 3.3V Application (Circuit Shown in Figure 1)

and ISN pins does not exceed 50mV. The ICTRL pin allows the user to control this limit between 0mV and 50mV by applying 0V to 1V to the ICTRL pin. The IMON pin outputs a ground-referenced voltage that is 20 • (ISP – ISN), which allows easy monitoring and may be used as an input to an A/D.

The LT8611 current sense and monitoring functionality may be used to limit short-circuit current or to create constant-current, constant-voltage (CCCV) supplies. Figure 3 shows well controlled current during a short-circuit event. The LT8611 can also be combined with a microcontroller with A/D and D/A to create sophisticated power systems. Typical apps include maximum power point tracking (MPPT) for solar charging and programmable LED current source.
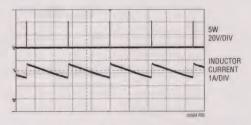

Figure 3. Short-Circuit Current is Well Regulated at 42V with the LT8611

Wide Input Range Operation at 2MHz

It is well known that higher switching frequencies allow for smaller solution sizes. In fact, a 2MHz switching frequency is often used in automotive applications to avoid the AM band and minimize solution footprint.

High switching frequencies, though, come with some trade-offs, including reduced ability to handle wide input voltage range commonly found in automotive and industrial environments. However, the LT8610 and LT8611 minimize these restrictions by allowing both high switching frequencies and high conversion ratios. This is due to their low minimum on-times (50ns typical) and low dropout, resulting in a wide input range, even at 2MHz. Figure 4 shows a 5V, 2A, 2MHz circuit that can accept 5.4V to 42V inputs. The circuit has a 2A output current limit.
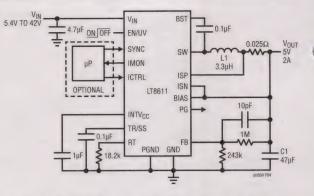
Figure 4. LT8611 Running at 2MHz Reduces Solution Size, Avoids AM Band, and Still Allows High Duty Cycle

Low Dropout Operation

As the input voltage decreases toward the programmed output voltage, the LT8610 and LT8611 maintain regulation by skipping switch-off times and decreasing the switching frequency up to a maximum duty cycle of 99.8%. If the input voltage decreases further, the output voltage remains 450mV below the input voltage (at 2A load). The boost capacitor is charged during dropout conditions, maintaining high efficiency. Figure 5 shows the dropout performance.

Figure 5. LT8610/LT8611 Dropout Performance

Conclusion

LT8610 and LT8611 are 42V, 2.5A synchronous step-down regulators that offer 2.5µA quiescent current, high efficiency, fault robustness and constant current (LT8611 only), constant voltage operation in small packages. This combination of features makes them ideal for the harsh environment commonly found in automotive and industrial applications.

For applications help,
call (408) 432-1900, Ext. 3513

Figure 2 You can further analyze the data by zooming in on the free-fall signal.

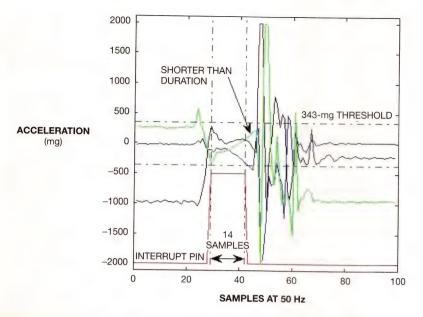pressure sensor's altitude detection to detect whether a hospital patient has fallen. If the sensor confirms a fall, the medical device's host processor sends an alarm to hospital personnel through a wireless link. The latest small accelerometers and pressure sensors with ultralow-power consumption have enabled such "man down" applications because the battery-operated medical devices are power-sensitive.

By definition, free fall is a state during which there is no application of external force, except for Earth's gravity, to the accelerometer. Theoretically, a three-axis accelerometer simultaneously outputs 0g measurements for all of its sensing axes during free fall; thus, other motions cannot "fake" the free-fall event. When someone throws an object upward, the object is in free fall from the moment of the throw. If an accelerometer is located away from the rotation center of an object, centrifugal force will cause the accelerometer to output no g force during the free fall. It is prudent, therefore, to install an accelerometer at the device's rotation center for free-fall application.

Most accelerometer manufacturers calibrate and test the devices in their factories, so users need not perform any further calibration after mounting the devices on boards for free-fall detection. The 0g offset of the accelerometer may be within ±40 to ±100 mg, how-ever, because the manufacturer might not horizontally mount the accelerometer after PCB assembly. Because of that offset, you may need to configure the accelerometer's threshold and time parameters to prevent false free-fall detection and avoid missing the real free fall.

To configure an accelerometer for free-fall detection, you can use the evaluation board of a three-axis digital accelerometer. The accelerometer's evaluation board and its Windows demo software capture the device's raw data and the interrupt signal (**Figure 1** and **Reference 1**); you can further analyze the data by zooming in on the free-fall signal (**Figure 2**). The accelerometer operates at a 50-Hz output-data rate, ±2g full-scale range. The interrupt registers simultaneously represent AND logic for x-, y-, and z-low detection plus or minus a 343-mg threshold and a 40-msec duration.

The designers first hold the accelerometer evaluation board at a random orientation and then drop it to the floor. As **Figure 1** shows, the device successfully detects the free-fall interrupt. The positive and negative peaks indicate the time that the board hit the floor. As **Figure 2** shows, the accelerometer's raw data on the x, y, and z axes entered the threshold zone for at least 40 msec, or two samples, generating the free-fall interrupt, and the free fall

lasts for 14 samples, or 280 msec. After the interrupt signal becomes low, the raw data on the x, y, and z axes again fall into the threshold zone, though that condition does not last for 40 msec and thus does not generate a free-fall interrupt.

The user must determine the threshold and duration for the requirements for a free-fall-detection application.

WAKE-UP INTERRUPT

It is crucial to minimize power consumption for each component in a battery-operated device. When the magnitude of the raw data of the accelerometer's x, y, and z axes is approximately 1g for a certain amount of time, the device is stationary or inactive (**Reference 2**). You can use the inactive state to switch off the LCD screen of a smartphone to save power, for example. In contrast, when you apply motion to the smartphone, the accelerometer can generate a wake-up interrupt to switch on the LCD screen.

The wake-up interrupt employs OR logic, rather than AND logic, which means that at least one of the acceleration data points on the x, y, or z axis is beyond the preset threshold. You can use the accelerometer's built-in highpass filter to filter out the constant component of the acceleration.

For example, a wake-up interrupt with an acceleration threshold of 250 mg corresponds to approximately ±14.5° of tilt angle. If a device tilts at a larger angle or has applied acceleration larger than the threshold for at least the preset time, the system will generate an interrupt for one output-data-rate period. You can enable the interrupt latch bit to make the interrupt signal remain high at all times. Once the system reads the interrupt-status register, the interrupt signal returns to a low state.

SINGLE- AND DOUBLE-CLICK INTERRUPTS

Some digital MEMS accelerometers can generate single- and double-click interrupts and indicate the direction of the click motion. This feature has become increasingly attractive in portable devices such as smartphones, tablet PCs, watches, and e-book readers. Once the accelerometer generates the interrupt, the host processor can trigger functions in those devices.

Click-motion detection depends on the device's shape and material and the accelerometer's location in the device. Waving or shaking the device can cause a false click motion. Therefore, you must fine-tune the accelerometer's settings for click-interrupt generation to detect the actual click motions and reject the false ones reliably.

The host processor's timer defines the double-click time, or the duration allotted for two successive, single-click events. If the second single-click interrupt happens within this time, the host processor knows that a double-click event has occurred. Otherwise, it still considers the event as a single click.

To get a reliable single-click interrupt, you must configure the click threshold and the time limit. When the acceleration is beyond the threshold, the accelerometer starts counting the number of samples or the elapsed time. The accelerometer generates the interrupt only when the acceleration falls below the threshold within the preset time limit.

You can latch the single-click interrupt by enabling a certain bit in a dedicated click-interrupt register. Once the system has read the click-status register, the device clears the interrupt signal and obtains the direction of the click motion.

Windows demo software and the accelerometer evaluation board capture the image of these tasks (**Figure 3**). The accelerometer is at ±4g full-scale and a 1250-Hz output-data rate. The click threshold and time limit are 2.25g and 1.6 msec, or two samples at that output-data rate, respectively. At ±4g full-scale, the sensitivity of the accelerometer's raw data is 2 mg/LSB (least-significant bit). The higher the output-data rate is, the more reliable the rejection of false motions will be. A higher output-data rate also consumes more power, however, representing a trade-off between single- and double-click implementations.

When Sample 14 in **Figure 3** is beyond the threshold, the accelerometer starts counting. Sample 15 is still beyond the threshold, whereas the acceleration falls below the threshold before Sample 16, which is the time limit; thus, the accelerometer generates an interrupt at Sample 16. The acceleration on the x axis crosses the negative threshold, and the value in the click-status register shows that the single-click motion thus corresponds to the direction of the x axis.

As you can see, accelerometers can be configured to monitor the acceleration on three axes in the background while the host processor performs other tasks or simply stays in sleep mode. You can use the acceleration data to implement accelerometer-interrupt features, such as data ready, free fall, wake-up, single click, and double click.

MEMS accelerometers measure linear acceleration but cannot distinguish among different types of motion. To

implement reliable and robust interrupt-based applications, including screen rotation, position orientation, and single- and double-click detection, the host processor must read and process the accelerometer's raw data using the requirements of each application.

Future MEMS accelerometers will have more built-in advanced features and computing capabilities to generate those interrupts reliably and to offload data processing from the external host processor.**EDN**

ACKNOWLEDGMENT

REFERENCES

1 "STEVAL-MKI022V1: MEMS 3-axis ±2g/±4g/±8g smart digital output evaluation board based on nano accelerometer LIS331DLH," STMicroelectronics, http://bit.ly/KWZ58e.

2 "AN3182: Tilt measurement using a low-g 3-axis accelerometer," STMicroelectronics, April 2010, http://bit.ly/JuxoEo.

AUTHORS' BIOGRAPHIES

Jay Esfandyari is a MEMS-product-marketing engineer at STMicroelectronics. He is the author of many papers and articles on MEMS technologies, products, and applications. Esfandyari holds master's and doctorate degrees in electrical engineering from the University of Technology of Vienna (Austria). You can reach him at jalinous.esfandyari@st.com.

Gang Xu, senior application engineer at STMicroelectronics, has more than 10 years of experience in the application of MEMS accelerometers, gyroscopes, and magnetometers. He received a doctorate in electrical engineering from Shanghai Jiao Tong University (Shanghai) in 1996.

Paolo Bendiscioli is an application manager for the motion-MEMS division of STMicroelectronics and has more than 10 years of experience in the applications of MEMS accelerometers, gyroscopes, and magnetometers. He is responsible for the application-development and customer-technical-support teams. Bendiscioli received a degree in electronics engineering from the University of Pavia (Italy) in 1997.

designideas

READERS SOLVE DESIGN PROBLEMS

Simple automatic-shutoff circuit uses few components

Noureddine Benabadji, University of Sciences and Technology, Oran, Algeria

▼ You often need to include a timed automatic-turn-off circuit in battery-powered equipment to extend battery life. Previously published Design Ideas for this function all involve many components (references 1 through 7). The circuit in Figure 1 is a simple automatic-shutoff add-on circuit featuring no quiescent current.

When you press the pushbutton switch, C_1 charges rapidly through the low-value R_2 to the zener voltage of diode D_1, and P-channel MOSFET Q_1 immediately conducts. After the pushbutton is released, C_1 discharges slowly through the high-value R_1 with a time constant of R_1C_1 seconds. During this

time, C_1 loses 63% of its initial voltage—from 9V to 3V after the delay. Reference 8 shows the on-resistance versus the gate-to-source voltage of a Vishay Siliconix Si4435. As long as the gate-to-source voltage is greater than approximately 3V, the device's on-resistance remains lower than 0.1Ω, yielding a dropout voltage of less than 0.1V for a load sinking as much as 1A.

The 9.1V zener diode, D_1, keeps the shutoff time delay independent of the battery voltage and ensures that the gate-to-source voltage does not exceed Q_1's rated maximum of 20V. Thus, you can use this circuit with a choice of battery voltages; only the maximum

drain-to-source voltage of transistor Q_1 limits the choice. With 3.6 to 9V batteries, D_1 and R_1 are useless (remove D_1 and short-circuit R_2), and you must compute the time delay with the classic **equation** $T = -R_1C_1\log_e(3/V_{BAT})$, as **Table 1** shows. With battery voltages as low as 1.5V, instead use a bipolar transistor with a low saturation voltage as well as a modified circuit scheme.

Editor's note: With no feedback for rapid shutoff, as C_1 slowly discharges below 3V, Q_1 goes through a period of gradually increasing the on-resistance, which temporarily increases its power dissipation and heating during the shutoff action. Be sure to consider this effect, size Q_1 adequately for the load current, and use adequately sized heat sinks.**EDN**

Figure 1 This simple automatic-shutoff circuit uses a P-channel MOSFET.

TABLE 1 TIME DELAY (SECONDS) WITH 10-MΩ R_1

Battery voltage (V)	LN $(3/V_{BAT})$	C_1=10 µF	C_1=100 µF
7.5	−0.916	92	916
6	−0.693	69	693
4.5	−0.405	41	405
3.6	−0.182	18	182

REFERENCES

1 Baddi, Raju, "CMOS gate makes long-duration timers using RC components," *EDN*, March 1, 2012, pg 43, http://bit.ly/H9zt6n.

2 Chenier, Glen, "RC-timed shutoff function uses op amp and momentary switch," *EDN*, Feb 16, 2012, pg 45, http://bit.ly/HaSryz.

3 Espí, José M; Rafael García-Gil; and Jaime Castelló, "Circuit extends battery life," *EDN*, July 29, 2010, pg 42, http://bit.ly/Hc9zED.

4 Xia, Yongping, "Battery automatic power-off has simpler design," *EDN*,

March 31, 2005, pg 80, http://bit.ly/bLJNgb.
5 Gimenez, Miguel, "Scheme provides automatic power-off for batteries," *EDN*, May 13, 2004, pg 92, http://bit.ly/aUdD3s.
6 Xia, Yongping, "Timer automatically shuts off," *EDN*, Aug 17, 2000, pg 128, http://bit.ly/GRefMO.
7 Elias, Kamil, "Timer provides power-off function," *EDN*, May 22, 1997, http://bit.ly/MlbQxg.
8 "Si4435BDY P-Channel 30-V (D-S) MOSFET," Vishay Siliconix, May 4, 2009, http://bit.ly/HaWjiZ.

Inverting level-shift circuit has negative potential

Chun-Fu Lin and Shir-Kuan Lin, National Chiao Tung University, Hsinchu, Taiwan; and Hui-Shun Huang, Jyi-Jinn Chang, and Tai-Shan Liao, National Applied Research Laboratories, Hsinchu, Taiwan

Digital-system designs require you to consider many core voltages. Memory operates at 1.8V, I²C and FPGA devices operate at 3.3V, microcontrollers operate at 5V, and charge-coupled-device image sensors operate at −9 to 8V. Clocks for each device must suit their operating voltages.

You can use the level-shift circuit in **Figure 1** to adjust an input clock signal to the proper logic-high and logic-low voltage levels, including negative voltages. This property is handy for devices that need a negative voltage, such as a charge-coupled-device sensor. Although the circuit's output clock is 180°-inverted relative to the input clock, that inversion does not affect the function of the device.

The level-shift circuit comprises fast-switching transistors Q_1 and Q_2. The user chooses level-shift high and level-shift low, which are dc-bias voltages and which connect to the transistor emitters, to match the desired output high- and low-logic levels. C_1, R_1, D_1, C_2, R_2, and D_2 keep the base voltages of Q_1 and Q_2 close to that of their emitters.
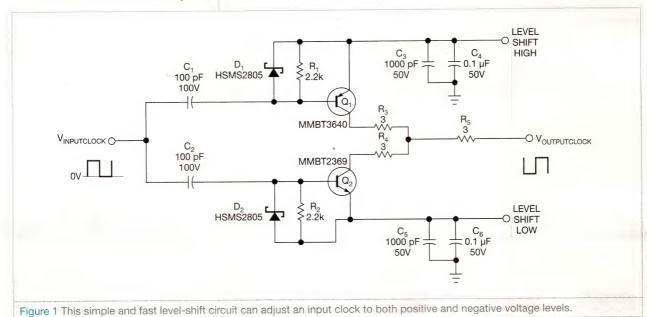
Because memory and charge-coupled-device sensors usually have high-frequency clocks, you can choose C_1 and C_2 to prevent low-frequency-noise pass-through. The circuit in **Figure 1** uses a 20-MHz signal for measurements (**Table 1**) and thus uses a value of 100 pF for C_1 and C_2. When the input voltage's clock is low, Q_1 turns on and Q_2 turns off, driving the output voltage's clock to the level shift's high potential. When the input voltage's clock is high, Q_1 turns off and Q_2 turns on, driving the output voltage's clock to the level shift's low potential, even when that potential is negative relative to ground.

Because of the circuit's high switching speeds, keep component leads as short as possible to minimize inductance. This caveat is especially true for C_3 through C_6's leads to their respective transistor emitters and to the ground plane or the output ground return.**EDN**

TABLE 1 INPUT AND OUTPUT CLOCKS

High/low level shift (V)	Input clock (V)	Output clock (V)
3.3/0	0/5	3.3/0
20/10	0/5	20/10
−5/−10	0/5	−5/−10
2/−4	0/5	2/−4

Figure 1 This simple and fast level-shift circuit can adjust an input clock to both positive and negative voltage levels.

Single hex-inverter IC makes four test gadgets

Raju Baddi, Tata Institute of Fundamental Research, Pune, India

This Design Idea describes a simple way that you can use one hex-inverter package of an unbuffered HD14069UB CMOS (**Reference 1**) to make four test gadgets: a logic probe with well-defined logic-voltage windows and with an input impedance of approximately 1 MΩ; a continuity tester whose upper limiting resistance can be tens of ohms to tens of megohms; a single or train pulse injector or a modest signal generator; and a high-impedance audio probe. You can assemble these gadgets using the six inverter gates of a 4069, two or three transistors, and a few passive components.

In a two-gate CMOS/TTL-compatible probe, the resistor network comprising R_1 through R_4 biases the inverter's inputs (**Figure 1**). Because of the gates' high input impedance, R_1 through R_4 can have values of approximately 100 kΩ to 1 MΩ. The probe's source/sink current is small at the probe tip because of the high resistances of R_1 through R_4; as a result, the probe tip essentially does not affect the logic-voltage level at the test point. Knowing the gates' input threshold voltage, you can calculate the required values of resistors R_1 through R_4.

The upper gate detects logic zero, and the lower gate detects logic one. Set an upper limit to the logic-zero voltage and calculate the values of R_1 and R_2. Arbitrarily select R_1=1 MΩ and seek a value for R_2 such that the voltage at the input of the upper gate is just the threshold voltage. Thus, $R_2=R_1(V_T-V_L)/(V_S-V_T)$, where V_T is the threshold voltage, V_L is the logic-zero voltage, and V_S is the supply voltage. Similarly, set a lower limit on the logic-one voltage V_T and seek a value for R_4 in terms of R_3. By appropriately selecting R_3, keeping in mind the quiescent biasing of the gates to keep both the LEDs off in the probe's suspended condition, you can obtain the value of R_4: $R_4=R_3V_T/(V_H-V_T)$.

The following **equation** calculates the probe current: $I_P=[-(V-V_1)(R_3+R_4)+V_1(R_1+R_2)]/(R_1+R_2)(R_3+R_4)$, where I_P is the probe current and V_1 is the probe-tip voltage. It thus follows that the probe impedance for any voltage at the probe tip is greater than 1 MΩ. For packages of 4069 that exhibit a larger threshold voltage, such as 3V, you can help reduce it by including a diode followed by a 10-kΩ load resistor to ground in the positive supply rail to the chip.

Developers often use continuity testers (**Figure 2** and **Reference 2**) as elementary test gadgets; such testers are indispensable on a work bench. One of the 4069's gates, with its high input impedance and with a threshold voltage for the transition of the output of the gate, allows you to build the continuity tester with an upper limit on the resistance of the test circuit. The total of the resistance between the probes and resistance in the switching arrangement forms a voltage-divider network, producing a voltage at the input of the gate. When the two resistances are equal, the voltage at the gate input is half the supply voltage. The transition threshold voltage of the gate is also nearly half the supply voltage; therefore, the selected resistor in the switching branch sets the approximate threshold-continuity resistance.

A useful alternative arrangement is to have a variable resistor in place of the switchable resistors. This approach allows you to set the threshold-continuity resistance arbitrarily by adjusting this resistor after including the desired resistance between the probe tips and observing the LED's glow. The variable resistor
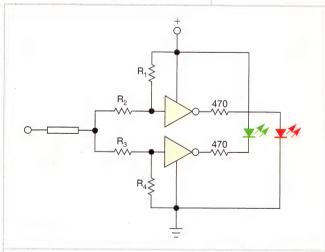

Figure 1 You can make a logic probe TTL/CMOS-compatible using just two gates from a single unit of an HD14069UB hex inverter. The suggested values for threshold and supply voltages are 2.5 and 5V, respectively; those for R_1, R_2, R_3, and R_4 are 1 MΩ, 680 kΩ, 200 kΩ, and 1 MΩ, respectively.
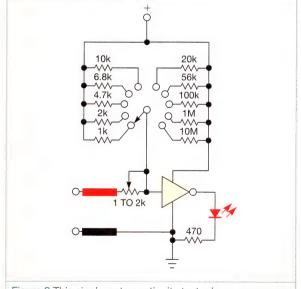

Figure 2 This single-gate continuity tester has an adjustable detection threshold.

designideas

should be set so that the LED just goes off. This method results in a compact arrangement, which a small package can accommodate. Another variable resistor (1 to 2 kΩ) is included in series with the negative probe to make it possible to have a threshold-continuity resistance of approximately 100Ω or less. You can also use a lower transition threshold voltage for the gate by including a couple of diodes followed by a 10-kΩ load resistor to ground in series with the positive supply rail. This arrangement can also be used to test for live ac-mains lines (**Reference 3**) with suitable modification, virtually making five gadgets.

Three gates still remain in the 4069 package; you can use two of them to make an astable oscillator/monostable single-pulse-generator circuit, which a complementary bipolar pair buffers to

increase the drive current (**Figure 3**). You select between a single pulse or a pulse train with an SPDT (single-pole/double-throw) switch set to P (pulse) or A (astable). In pulse mode, pressing the switch produces a brief negative-going pulse at the input to the second gate as C_2 begins charging. The resulting high at the gate output causes a positive-going pulse at the junction of Q_1 and Q_2. It also is latched, and the switch is debounced by the positive feedback through capacitor C_1, which begins charging at a time constant that the selection of R_1, R_2, or R_3 determines. When the voltage across C_1 equals the threshold voltage, the second gate output returns low, again with positive feedback through C_1, driving the second gate input high and ending the pulse.

The diode in parallel with C_2 is

always reverse-biased and serves as a very large-value resistor to discharge C_2. Assuming a typical diode leakage of 1 nA, the equivalent resistance at 2.5V is about 2.5 GΩ. The RC discharge time constant of approximately 125 msec is suitable for the human rate of pushing the button.

The values of R_1 through R_3 set the astable frequency or the one-shot's pulse width. The 220-kΩ resistor at the input of the second gate is included to limit the leakage of current from the capacitor into the gate input when its voltage is below that of ground or higher than V_{DD} by 0.6V. The astable produces a frequency of approximately $1/(2.2RC)$, whereas the threshold voltage of the gate determines the pulse width of the one-shot, which is approximately 0.7 to 1.1RC.

It is sometimes useful to listen to an audio signal at a test-circuit point. The 4069, with its high input impedance and sufficient output drive current of approximately 6.8 mA, can drive a small PCB-mountable speaker. That approach lets you build a simple audio probe (**Figure 4**). The resistor at the gate input of **Figure 4a** protects the gate if the unit under test has voltages higher than the gate supply voltage.

Two methods of driving the acoustic transducer are shown, depending on the loudness requirements. **Figure 4a** shows a direct connection to a piezo transducer. For the louder sound of a speaker, a small resistor can be added in series with the speaker of **Figure 4b** to control volume and prevent possible speaker or transistor damage. **Figure 4c** shows an optional method of biasing the gate input for enhanced sensitivity.

The biasing voltage is given by the voltage divider network using this equation: $V_B = R_2 V_S/(R_1+R_2) - R_2 V_L(1-\xi)/(R_1+R_2) - R_2 V_H \xi/(R_1+R_2)$, where V_S is the supply voltage, ξ is the duty cycle $(T_H/(T_H+T_L))$ of the input signal (assumed to be a rectangular wave), V_H is the logic-high voltage, and V_L is the logic-low voltage. A suggested value for R_1 is 1 MΩ; the user can choose

Figure 3 A complementary bipolar pair boosts the output current of the oscillator and the single-pulse generator.
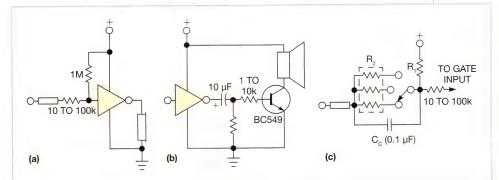

Figure 4 A resistor at the gate input protects the gate if the unit under test has voltages higher than the gate supply voltage (a). A small resistor can be added in series with the speaker to control volume and prevent possible speaker or transistor damage (b). In an optional method of biasing the gate input for enhanced sensitivity, various R_2 values are possible (c).

R_2 (suggested to be 1 MΩ) according to the **equation** for biasing voltage. Various R_2 values are possible, as the switching arrangement in **Figure 4c** shows. Capacitor C_C (suggested to be 0.1 μF) acts in series with the signal to be investigated and supplies the biasing voltage in series with the signal. The minimum strength of the signal is limited by the input threshold window of the gate and is different for different logic gates. For a rectangular signal changing between zero and the signal voltage, for example, the biasing voltage should be below the threshold window, and the value of the biasing voltage plus the signal voltage should be above the threshold window.

A stringent situation exists when those two values lie just at the edge of the window. So, for a rectangular or attenuated digital signal, $V_{SIG}=\Delta V_T$ is the minimum required signal strength. In general, gates differ in ΔV_T; some have wide widths (CD4069) and others narrow widths (CD4011). When an ac signal such as a sine wave is applied, however, the negative phase of the signal reduces the biasing voltage by its strength to V_B-V_{SIG}. It is thus sufficient that one phase produces a change equal to half of the window width. For ac signals, therefore, the minimum signal-strength criterion is $V_{SIG}=\Delta V_T/2$.

Finally, for an inverting gate, $\Delta V_T=V_{T2}-V_{T1}$, where V_{T2} is the input voltage at which the output of the gate has completely settled to logic zero, and V_{T1} is the input voltage at which the output of the gate has completely settled to logic one. R_1 and R_2 help in choosing the critical signal strength above the minimum that the threshold window of the gate has set. If R_2 is approximately 1 MΩ, then the R_2C_C time constant is 0.1 sec, which corresponds to 10 Hz and seems to be adequate.

For plain digital signals, it is enough to omit R_2 and C_C; in other words, both R_2 and C_C equal zero. It should be noted that this coupler does not remedy the stagnant signal condition, preventing a constant drain current at the output. It is intended to provide a typical transistor amplifier kind of biasing for the audio probe gate. The stagnant signal condition is taken care of with a series 10-μF capacitor at the gate output of **Figure 4b**.
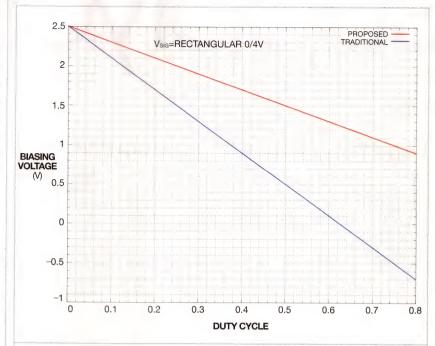

Figure 5 The input ac coupling of Figure 4c is less sensitive to duty cycle than is traditional series-capacitor ac coupling.

Readers interested in using the traditional ac coupling (with the left terminal of R_2 connected to ground instead of the probe tip) RC circuit may use the following formula to calculate the expected V'_B as a function of various parameters: $V'_B=V_S R_2/(R_1+R_2)-\xi(V_H-V_L)-V_L$, where all of the terms have the usual meaning.

Compare this **equation** with the previous **equation**. Whereas the biasing voltage in the **equation** for V'_B depends on V_H or V_L through a single multiplicative factor of the duty cycle, in the **equation** for the biasing voltage it depends on another multiplicative factor, $R_2/(R_1+R_2)<1$, thus reducing the dependence and producing a flatter profile with a duty cycle as shown in **Figure 5** for a rectangular wave of $V_L/V_H=0/4V$ and a varying duty cycle.

You can assemble all of these gadgets in a small container, such as a glue-stick tube, and use the probe for a variety of tests (**Reference 4**). You can power the probe using two 3V CR2032 lithium cells; the CMOS 4069 is a low-power device. Note, however, that 4069 devices from different manufacturers differ widely in their threshold voltages, so you should check that value before selecting a device to make the test

gadgets, especially the first three.

The key to these test gadgets is the high input impedance of the CMOS gates. Other packages, such as the CD4011/4001, can also yield multiple gadgets because what matters is the use of the inverter gate.

Editor's note: In all of the circuits discussed here, the probe ground should be connected directly to the unit-under-test ground. Although the Design Idea does not discuss it, some readers might want to add CD4011/4001 NAND/NOR logic to combine the continuity tester, astable oscillator, and audio probe to provide an audio tone for the continuity tester.**EDN**

REFERENCES

[1] Funk, RE, "Understanding Buffered and Unbuffered CD4xxxB Series Device Characteristics," Texas Instruments, 2002, http://bit.ly/LJbG5Y.

[2] Baddi, Raju, "Test continuity with an LED," *EDN*, Jan 6, 2011, pg 47, http://bit.ly/LkaWyk.

[3] Baddi, Raju, "Detect live ac-mains lines," *EDN*, Nov 4, 2010, pg 48, http://bit.ly/KOCErf.

[4] Baddi, Raju, "Probing system lets you test digital ICs," *EDN*, June 21, 2012, pg 48, http://bit.ly/NhOPgz.

supplychain
LINKING DESIGN AND RESOURCES

Questions linger on anti-counterfeit rules

The US government is expected in September to start issuing regulations to carry out the anticounterfeiting provision in the 2012 National Defense Authorization Act. A Senate Armed Services Committee investigation that found more than 1,800 instances of counterfeit electronics in the DOD (Department of Defense) supply chain prompted the provision.

Under the provision's terms, contractors can't charge the DOD for remediating problems related to counterfeit parts. The DOD and its contractors must buy electronic components from OCMs (original-component manufacturers), their authorized distributors, or "trusted suppliers" wherever possible, and contractors must establish policies to "eliminate" counterfeit electronic parts from the supply chain.

Henry Livingston, an engineering fellow and technical director at BAE Systems and one of the speakers at a recent symposium on counterfeit electronics, identified several aspects of the provision that will likely prove challenging. The term "eliminate," for example, is definitive but might be difficult to achieve in practice, he said.

The provision is unclear regarding responsibility for remedial costs. It doesn't define what a remedy is or how much responsibility a company must assume for costs. The provision does not focus on where the component enters the supply chain, and it lacks requirements for independent distributors or OCMs to help support the identification of counterfeits.

Nothing in the provision addresses what contractors are supposed to do with counterfeits they discover. The logical decision would be to return them for a refund, but counterfeit parts should not be put back into the supply chain, where they can then be sold to others.

The government was expected to define several terms and offer guidance on how suppliers should report counterfeits. As of June 27, however, there had been no word. By the end of September, the DOD is supposed to propose regulations that outline specific contractor responsibilities. Without those details, companies can't accurately assess how well they'll be able to meet the requirements.—**by Tam Harbert**
This story was originally posted by EBN: *http://bit.ly/P3OAaw.*

CONTRACT MANUFACTURERS CAPITALIZE ON SHIFT TO ULTRABOOKS

With their main business in notebook PCs under pressure, ODMs (original-design manufacturers) are adding new capabilities that will allow them to capitalize on the soaring sales of ultrabooks, according to research firm IHS.

"ODMs now are hoping to jump in on the action on ultrabooks, predicted to be the next big growth sector in computing, by securing the casings for anticipated future ultrabook orders," says Thomas J Dinges, CFA, senior principal analyst for EMS and ODM research at IHS.

Casing companies sell metal cases that serve as the frames of electronic devices. To date, Taiwan-based Compal Electronics Inc has invested tens of millions of dollars in joint ventures with casing suppliers in China to support the needs of its notebook customers. Overall, the major notebook ODMs will attempt to procure up to 10,000 machines in 2012 for their casing-manufacturing operations and joint ventures.

With the production of ultrabooks expected to ramp up and Apple's sales continuing to grow, casing supplies will remain tight for the near term, IHS believes.
—**by Amy Norcross**

GREEN UPDATE

MEDICAL TO FALL UNDER ROHS SCOPE IN 2014

If you think ROHS is in your rearview mirror, think again. A significant electronics market is going to feel the impact of the ROHS directive within the next few years and may be caught unprepared.

Medical devices will fall under the scope of the ROHS directive starting in 2014, according to Gary Nevison of Newark/Element14. Medical devices have so far been exempt from ROHS because of the critical nature of the devices and the necessary use of hazardous materials, such as lead, to protect users from radiation. The sale of noncompliant devices into the European Union won't be halted until 2019.

The manufacture of medical devices is still a very tightly held business. It is highly regulated, and it is difficult to quality for the various approvals required by law. Medical-electronics companies have also been slow to outsource manufacturing, preferring to retain quality control in-house. Now that medical devices will fall under ROHS, that sector will likely experience many of the same issues the broader industry has encountered in interpreting and implementing the directive's requirements.

Medical equipment companies can continue to ask for exemptions to the rule.—**by Barbara Jorgensen, *EBN* community editor**
This story was originally posted by EBN: *http://bit.ly/LWb11u.*

FLEXIBILITY.

DESIGN CHAIN SOLUTIONS FROM AVNET

You think about innovation, we think about the rest.

Our team of engineers has the right mix of technical skills and application experience to give you the support you need – throughout the design chain. Extensive technical support, FPGA design, and world-class training. That's what the No. 1 in design support can do to help you focus on what you do best and successfully compete in the global market. Our solutions bend to meet your needs.

What can we do for you? www.avnetexpress.com

Accelerating Your Success!™
1 800 332 8638 | www.avnetexpress.com | [f] [t] @avnetdesignwire

AVNET®
electronics marketing

productroundup

COMPONENTS AND PACKAGING

Vishay panel potentiometer targets low-profile, low-weight equipment

The Sfernice P16S potentiometer features a unique knob driving that incorporates a cermet or conductive-plastic potentiometer. Mounting hardware and terminals are placed on the panel's back side, providing for a minimum clearance and use in small, low-profile, low-weight equipment. The power rating is 1W at 40°C. TCR is ±150 ppm/°C typical, and dielectric strength is 2.5 kV_{RMS}. The P16S is available in a 7-mm bushing length with a 16-mm knob diameter and a temperature range of −40 to +125°C. Samples are available now, as are production quantities, with lead times of eight to 10 weeks for larger orders. Pricing starts at $6 per piece (1000) for US delivery.
Vishay Intertechnology, www.vishay.com

Stackpole axial-leaded resistor features 2W power rating

The ASRM2 mini antisurge axial-leaded resistor has a voltage rating of 4 kV, with an overload voltage rating of 5 kV, and is rated for 2W of continuous power. The ASR series is designed to handle high-voltage pulses of up to 10 kV, depending on size and resistance value, for thousands of pulse events. The ASR has a flameproof coating per UL94 V-0 and is ROHS-compliant. The ASR/ASRM is designed as a suitable surge resistor for many power supplies, CRTs and other display types, small motor controls, security systems, industrial automation and control, snubbers, power-supply primary-side discharge resistors, and LED lighting. The series is suited for high-voltage applications, including medical devices, plasma cutters, welding equipment, personal-protection devices, power- and phone-distribution protection, and instrumentation. Pricing varies with size and resistance value, ranging from 5 cents to 12 cents each in full-reel quantities.
Stackpole Electronics, www.seielect.com

NXP MOSFETs have tin-plated, solderable side pads

The PMPB11EN and PMPB20EN 30V N-channel MOSFETs are housed in a 2×2-mm low-profile DFN (discrete flat no-lead) package with tin-plated, solderable side pads. The side pads offer optical soldering inspection and a better quality of solder connection compared with conventional leadless packages. The MOSFETs are the first of more than 20 devices housed in the DFN-2020MD-6 (SOT1220) package. Both devices have a maximum drain current of >10A and very low drain-to-source on-resistance values of 12 mΩ typical and 16.5 mΩ typical at 10V for reduced conduction losses, enabling lower power consumption and longer battery life. Measuring 0.6 mm in height, the DFN2020 MOSFETs are thinner than most 2×2-mm products and thus are suited for ultra-small load switches, power converters, and charger switches in portable applications such as smartphones and tablets. Eight times smaller than standard SO8 packages, the DFN2020 offers comparable thermal resistance and can

replace many larger MOSFET packages with the same drain-to-source-on-resistance-value range. Pricing starts at 20 cents (10,000) for the PMPB11EN and 16 cents (10,000) for the PMPB20EN. **NXP Semiconductors, www.nxp.com**

Cellergy CLC supercapacitors offer small footprint

The CLC series of supercapacitors offers low leakage current with its small-footprint (12×12.5-mm) product. Heights range from 2.4 to 3.6 mm. The maximum leakage current is 1.5 μA for single-cell and 3 μA for double-cell configurations. Used with batteries to deliver energy to the load, the supercapacitors target such applications as RFID tags, wireless alarms, medical systems, low-power transmitters, and remote controls. They are offered with 3.5, 4.2, and 5.5V nominal voltages; ESR values from 300 to 720 mΩ; and capacitance values from 10 to 25 mF. The price for the 12×12.5-mm-packaged devices is $1.70 (5000). Standard lead time is four to six weeks; availability is expected by July 30. **Cellergy, www.cellergycap.com**

Fairchild P-Channel MOSFETs minimize board space in mobile devices

The FDZ661PZ and FDZ663P P-channel, 1.5V-specified PowerTrench 0.8×0.8-mm WL-CSP MOSFETs feature state-of-the-art fine pitch and minimize board space and drain-to-source on-resistance for a miniature form factor. Packaging occupies 0.64 mm^2 of PCB area, less than 16% of the area of a 2×2-mm CSP. The ultralow profile has a height of less than 0.4 mm when mounted to the PCB. The devices are suitable for use in battery-management and load-switch functions in mobile applications. The ROHS-compliant MOSFETs offer a gate-to-source voltage as low as −1.5V. They are priced at 26 cents (1000). **Fairchild Semiconductor, www.fairchildsemi.com**

Littelfuse Micro3 blade fuses address tight spaces

The Micro3 line of blade fuses combines two individual fused circuits into a single subminiature body.

producteroundup

Less than 15-mm wide, the fuses offer the same 5-mm terminal spacing and electrical performance as single-fuse solutions. Each fuse is rated for high temperature (under hood) operation, with an operating temperature range from −40 to more than +125°C. The fuses also offer tighter overload tolerances and are available in four current ratings from 5 to 15A, with a 32V-dc rating and standard 2.8-mm terminals. The products allow for more circuits in a small space, decreasing harness weight and maximizing area. Pricing depends on volume; the devices are in production now.
Littelfuse, www.littelfuse.com

AVX TCJ high-voltage capacitors maintain 20% recommended voltage derating

The TCJ series SMDs (surface-mount devices) are the industry's first 63 and 75V single-anode tantalum polymer capacitors, according to the vendor. The capacitors deliver high capacitance, high voltage, and low ESR values in a small case size. Available in 1-μF/63V, 4.7-μF/63V, 10-μF/63V, 4.7-μF/75V, and 6.8-μF/75V rated voltages, they maintain 20% recommended voltage derating, extending the usable voltage range. The TCJ series capacitors maintain high reliability, exceeding 1% per 1000 hours at 85°C and full-rated voltage. They are suited for high-voltage applications, including ac/dc converters supplying circuits in LCD TVs, base stations, rectifiers, switching hubs, and router and line filters, as well as LED power drivers in PC monitors and LED TVs. The TCJ series is free of piezo issues related to the use of MLCC ceramic capacitors in circuits such as backlight controllers in LCD monitors and displays. The high-voltage tantalum capacitors also reduce the number of parts required because of their lower ESR, increasing layout flexibility. Lead time for the series is 10 weeks. Contact the company for prices.
AVX Corp, www.avx.com

Temp-Flex microwave coaxial cables provide fast signal speed

Microwave coaxial cables designed for high-bandwidth applications are available with a solid-core fluoropolymer-resin dielectric (low loss) or air-enhanced design with a fluoropolymer-resin layer applied over dual monofilaments (ultralow loss) around the center conductor for increased signal speed. The cables provide phase stability, impedance tolerance of 50 to ±1Ω, tight time-delay tolerance, an FEP alternative to PTFE and ePTFE, bandwidth potential to 110 GHz, and stability under dynamic conditions. All cable sizes have a helically wrapped, silver-plated copper and flat-wire shield and braid to achieve superior shielding effectiveness. Standard solid-core construction coaxial cable delivers 70% VOP (velocity of propagation); the air-enhanced design achieves 85% to 88% VOP and improved insertion loss at high frequencies. The standard-product family comes in 047, 086, and 141 sizes; prices are based on volume with a six-week lead time.
Temp-Flex LLC, www.tempflex.com

Vishay VJ MLCCs feature Q factor of 2000

The VJ HIFREQ series of high-frequency RF and microwave surface-mount MLCCs features high self-resonance; a high Q factor, of 2000; and a low dissipation factor, of <0.05%. The devices are optimized for filter and matching networks and for amplifier and dc blocking circuits. They are offered in 0402, 0603, and 0805 case sizes with working voltages from 25 to 250V dc. The capacitors have wide capacitance ranges, from 1 pF to 1.5 nF, and tight tolerances, to ±0.1 pF; an aging rate of 0% per decade; and an operating temperature range of −55 to +125°C. Pricing starts at 6 cents per unit.

Vishay Intertechnology,
www.vishay.com

This one really takes the cake— and the schematics

Early in my consulting career, a start-up company contacted me. It had designed a system for capturing medical images and sending them over a network. The product was behind schedule, so the venture-capital backers had fired the founder, and the hardware engineers had quit in solidarity. The company was left with a bunch of software engineers and hardware that didn't work; my job was to fix it. There was no documentation, and the original engineer had taken the schematics home and refused to return them. I had to reverse-engineer a PCB and an FPGA by observing the external signals with an oscilloscope and a logic analyzer.

I didn't find anything wrong with the logic, but I did find a lot of poor design practices, such as marginal timing, asynchronous logic, poor grounding, and missing signal terminations. I rewired the board, added termination resistors, strengthened ground connections, and even made changes to the FPGA by opening the internal routing files and manually rerouting signals and changing logic. The board passed all tests; the next step was to redesign it.

I discovered that the DSP manufacturer no longer supported the product and that the DRAMs were obsolete. I suggested redesigning with newer components, and everyone agreed, even though the software engineers would need to rewrite their low-level code.

After a month redesigning the board and a month for manufacture and assembly, the new board arrived. I asked the software engineers for their new code. They said they hadn't had time to rewrite any code because the venture backers had insisted on a completed demo by a certain date; otherwise, the backers would pull the funding. The company's CEO told me to redesign the hardware, putting back the obsolete components so that the current software would still run. I reluctantly complied.

By this time, the original design engineer had made friends again with management and told them my design wouldn't work. The CEO summoned me to his office, seeking reassurance. I had worked on this design so intently, reverse-engineering it without documentation, testing it, and redesigning it twice, that I gave him a guarantee: If the board didn't work, he wouldn't have to pay me. I added, though, that the board would have a half-dozen blue wires to correct minor problems.

The board came back on a Friday afternoon, and I started running tests. Around 8 pm, my memory tests started failing intermittently, even though all of the signals looked correct. In the DSP's data book, I read about the built-in DRAM controller. I was using the RAS-before-CAS (row-address strobe before column-address strobe) refresh mode of the memory, but I couldn't find that mode in the data book. It eventually sank in that the developers of this processor had designed it before that mode existed, so data just disappeared slowly.

With the company's future and my reputation on the line, I poured myself some coffee and let ideas float around in my head until a useful one surfaced. The processor was much slower than the rest of the board's circuitry. I had designed PAL (programmable array logic) chips into the board at several locations. I realized I could actually reroute the RAS and CAS signals from the DSP through the PALs, implement a state machine to create new RAS and CAS signals to the DRAM, and assert them periodically to refresh it. The DSP clock was so slow and the PALs so fast that I could slip in a refresh between normal accesses.

The reworked board consistently passed the memory tests. On Monday, I presented it to the CEO and told him I'd been wrong: "I said the board would work with a half-dozen blue wires, but I needed only four." **EDN**

Bob Zeidman is president and founder of both Zeidman Consulting and Software Analysis and Forensic Engineering Corp, both in Cupertino, CA.